CHARACTERIZATION OF SENSORY-MOTOR BEHAVIOR UNDER COGNITIVE LOAD

By

JIHYE RYU

A thesis submitted to the

Graduate School – New Brunswick

Rutgers, The State University of New Jersey

In partial fulfillment of the requirements

For the degree of

Master of Science

Graduate Program in Psychology

Written under the direction of

Elizabeth Torres

And approved by

_____

_____

_____

New Brunswick, New Jersey

October 2017

ABSTRACT OF THE THESIS

Characterization of Sensory-Motor Behavior under Cognitive Load

By JIHYE RYU

Thesis Director:

Elizabeth Torres

This thesis introduces a new experimental paradigm and offers a unifying statistical framework to characterize possible interdependencies among signals of the nervous systems through three proposed fundamentally different types of processes. We have coined the terms *deliberate*, *spontaneous* and *inevitable* for these processes. Deliberate processes manifest through overt movements executed during goal-directed actions (e.g., when instructed to point to a visual target). They are systematic in nature, and are well characterized by low variability and robustness to changes in bodily physical dynamics. Spontaneous processes manifest through highly automatic and covert movements, that are uninstructed and goal-less (e.g., retracting the hand from a visual target), and are characterized by high variability and susceptibility to environmental

cues and changes in bodily motion dynamics. These processes occur largely beneath the person's awareness, but can be brought up to conscious control when instructed to do so. They co-exist with, and are incidental to the goal-directed segments of complex motions, as they provide fluidity to behavior at large. The inevitable processes are generated by autonomic activities such as the heartbeat. They have a narrower range of change in dynamics and cannot be volitionally controlled or be perturbed by environmental cues, unlike the deliberate and spontaneous processes. These processes are robust and provide a unique signature of the person's nervous systems.

Here, we study these processes *in tandem* as participants perform a basic pointing task with different levels of cognitive load in the context of decision making. We assess the continuous somatic-motor performance of the nervous system through a personalized statistical analysis of the moment-by-moment fluctuations in the amplitude and timing of various biophysical parameters. These include variations in the amplitude of the angular acceleration peaks and their inter-peak interval timing, and variation in the inter-heartbeat-interval timings (IBI). We find that the interdependency is funneled out through one of the processes depending on the demands of the task. Tasks with differing levels of cognitive load manifest the interdependency through inevitable processes with shifts in the IBI stochastic signatures. Decision-making (a form of cognitive load) manifests the interdependency through deliberate processes with fluctuations in the amplitude of the angular acceleration peaks, and through spontaneous processes with the inter-peak interval variations. We emphasize that these findings do not refer to discrete mouse-clicks or verbally reported data. They are rather

in reference to continuous physiological data harnessed from the central, peripheral and autonomic nervous systems. As such, our methods are novel to the field of cognitive psychology. We discuss our results along with possible applications of this paradigm to basic science and clinical practices. Specifically, we invite their use in expanding the analytical tools for the nascent field of embodied cognition, and suggest these metrics to be used as dynamic outcome measures of voluntary, automatic, and autonomic control in clinical settings.

Acknowledgements

I would like to thank my mentor Dr. Elizabeth Torres, my committee members, Dr. Thomas Papathomas and Dr. Melchi Michel, and all the members of the Sensory-Motor Integration Lab for their help with my thesis.

This work was funded in part by the New Jersey Governor's Council for Medical Research and Treatment of Autism and the New Jersey Department of Health. It was also supported by the Nancy Lurie Marks Family Foundation Career Development Award to E.B. Torres.

Table of Contents

List of Tables

List of Illustrations

1. Introduction

1.1 Biorhythms as afferent/reafferent signals

The human body continuously generates biophysical rhythms throughout the multiply interconnected layers of the peripheral and central nervous systems (PNS and CNS), including the layers of the autonomic nervous systems (ANS) within the PNS. These biorhythms can be registered non-invasively by contemporary instruments that measure e.g., heart rate, respiration, brain waves (electroencephalography), muscle function (electromyography) and bodily kinematics, among others.

The waveforms of these biophysical rhythmic signals are generated and expressed as time series of peaks and valleys that fluctuate over time, as we naturally and continuously behave and move around. Such fluctuations can be understood as sensory feedback of consequence to the estimation and predictive planning of our self-generated actions and decisions. The central controllers in our brain are thought to utilize such information to build internal models for motor control in guiding a variety of cognitively registered processes [1-3]. For example, when we move in the dark, in the absence of any visual feedback, the kinesthetic/proprioceptive signals would allow us to perceive the changes in body positions over time, and in turn, motion representations from this feedback can be incorporated within the flow of conscious decisions to execute movement in a timely fashion.

Such afferent signals are necessary to execute any purposeful actions, because we would need to continuously sense the motions of the body, and update our motor and sensory maps based on the sensory flow. Indeed, in the words of Von Holst and Mittelstaedt [7], the

principle of reafference states that, "*Voluntary movements show themselves to be dependent on the returning stream of afference which they themselves cause.*"

To illustrate the importance of this principle in the context of kinesthetic reafference, we bring up the case of a deafferented subject Ian Waterman [8]. Ian transiently lost the ability to control his body due to a lack of kinesthetic reafference. His afferent fibers from the neck down were destroyed by a viral infection when he was 19 years old. Although his nervous system could produce efferent motor output to tense up the muscles across his body, without the continuous afferent feedback flow from his bodily motions, he could not move in any controlled fashion. His case is one of extraordinary importance in the field of neuromotor control because it demonstrates that sensory substitution of kinesthetic reafference by vision was possible through a combination of visual guidance and motor imagery. In the absence of proprioception, Ian learned to remap his sense of movement and the consequences of his movements by deliberately planning ahead every single bodily motion with the help of visually monitoring his limbs [9]. His brain regained the ability to compensate for sensory-processing delays, enabling him to better predict the sensory consequences of his impending action. Because Ian had already built sensory-motor maps in his brain by the age of nineteen (when the viral infection destroyed his afferent channels), he was able to rebuild a predictive code that connected external sources of sensory guidance with internal sources of guidance, anchored in a mental representation of his deafferented body (i.e., motor imagery). This representational map closed the sensory-motor feedback loops using the fluctuations of the rhythms from different biophysical channels.

It has been our proposition that in the process of executing movements using the closed feedback loop, we may have probabilistic maps of sensory consequences for impending motor actions and decisions. Such maps would be acquired by our brain through sampling the consequences of our physical acts through kinesthetic reafference, as well as other extraneous sources of sensory reafference, thus allowing for the development of representational and adaptive probability landscapes.

In fact, because biorhythms across multiple layers of the nervous systems are quantifiable, we know that their continuity and historicity are vital to the development and maintenance of a predictive code in our motor and sensory maps [10]. Along these lines, the variations produced by prior self-generated movements across multiple contexts accumulate probabilistic information that enables the nervous systems to generate subsequent movements in a well-informed manner. By sending the mixture of signals and noise embodied in the sensory motor priors to the brain (via afferent pathways), the past can influence the mixture of signals and noise generated by the subsequent movements (via efferent pathways), which would then transport a new set of signals and noise to the brain (via reafferent pathways).

1.2. Interdependency among Signals from Different Nervous Systems

The biophysical rhythmic signals within the multiply interconnected layers of the peripheral and central nervous systems (PNS and CNS) are in constant motion as we naturally behave. These signals may be interdependent with each other, or may be orthogonal with one another.

We posit that in order to develop and maintain *deliberate autonomy*, i.e. the ability to deliberately maintain a robust course of action on demand that is impervious to

external/environmental influences, interdependencies among biophysical signals from different nervous systems would be required. These interdependencies can be manifested by examining the inter-relations of three proposed processes: the deliberate, spontaneous, and inevitable processes (**Fig.1A**). These processes likely emerge from the interactions across the phylogenetically ordered structures and the functional neurophysiology of our nervous systems, including information processed by our sensory organs and information flowing through the efferent-afferent channels (**Fig.1B-C**).

Prior work concerning the neuromotor control of complex actions has used movement segments to examine the interplay between deliberate and spontaneous processes. Movement signals produced during natural behaviors are obtained from a blend of motion segments involving various levels of intent [4], spanning from those that are conscious and voluntary (i.e., high intent movements such as pointing at a screen) to those that are automatic and beneath the awareness (i.e., low intent movement such as rhythmical swaying of the arms while walking), as shown in **Fig.1B**. Deliberate processes map well onto voluntary goal-directed motions and spontaneous processes onto automatic uninstructed/goal-less motions, where the former is primarily driven by top-down processes from the CNS, generating biophysical rhythms that are more robust to changes in dynamics [4, 10, 13], while the latter is primarily driven by bottom-up processes, broadcasting different signatures of statistical variability [4, 10, 14]. Using this aspect of movement characteristics, recent studies have revealed that the statistical features of motor signals reflect the level of intent that is involved in complex sports behaviors [12], and these statistical features have been further explored among athletes *vs*. novices [4] and among individuals with autism spectrum disorders [5, 6].

At this point, inevitable processes from the ANS (unavoidable and impervious to volitional control) have not been characterized under a common statistical umbrella with deliberate and spontaneous processes. As such, there is an open question on whether peripheral biorhythms such as those generated by the heart in the ANS would also contain statistical information about cognitive activity, such as the level of intent. (**Fig. 1B-C**).

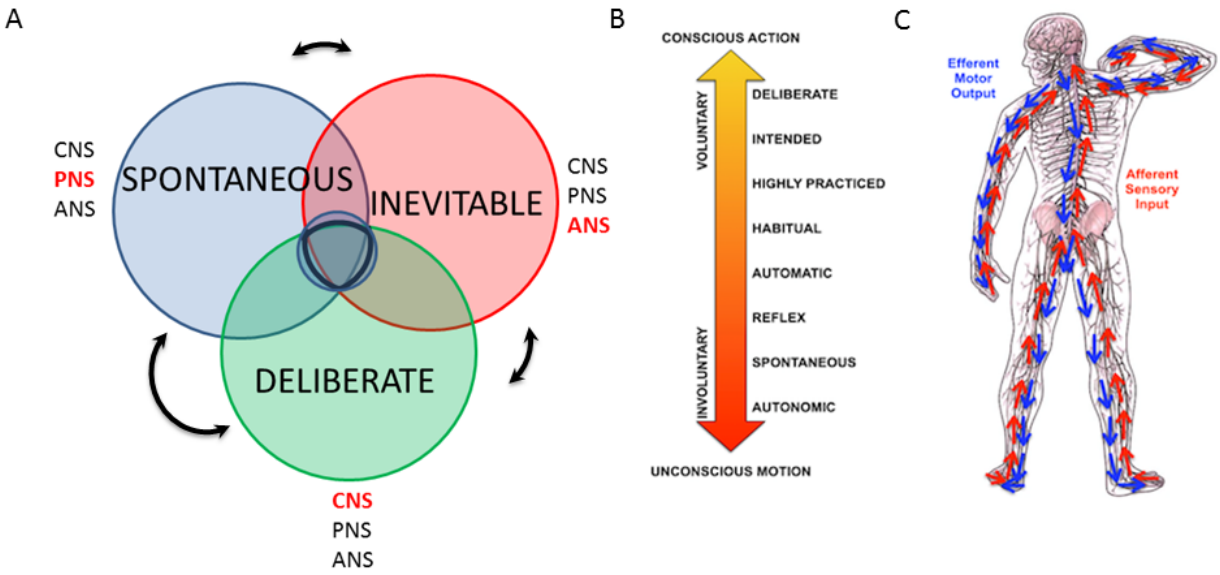

Figure 1. Interdependencies among signals from different nervous systems manifested through the proposed fundamentally different types of processes and the assessment of their roles through the statistical signatures of variability (statistical variability is explained further in section 2.4). (A) Proposed processes and the nervous systems that is predominantly involved in each of those processes, along with their interdependencies during natural behaviors that require cognitive decisions. A possible scenario is given here by the prevalence of the CNS on *deliberate* processes during voluntary goal-directed behaviors; the prevalence of the PNS instantiated through efferent-afferent influences on *spontaneous* processes manifested in uninstructed/goal-less motions, taking place beneath the person's awareness; the *inevitable* processes with a prevalence of the ANS involvement in e.g., rhythmic motions of the heart as an autonomic pacemaker underlying all actions. The shortness of the arrow connecting the inevitable process implies a narrower bandwidth of dynamics reflected within the ANS processes, supposedly due to the ANS system's stability and survival. (narrower bandwidth explained further in section 4.1) **(B)** A continuum from conscious to unconscious processes spanning the PNS and CNS, where each processes map onto different layers of statistical variability. **(C)** Bi-directional efferent (blue) and afferent (red) signals continuously flowing in closed loops between the central and the peripheral nervous systems with the underlying presence of the ANS. Extracted from [4, 11].

1.3. Embodied Approach

Since movement signals are a blend of deliberate and spontaneous processes with varying levels of intent, each layer of the nervous system would be contributing to the functionality of one's movement behavior with varying degrees, within the closed feedback loop of CNS and PNS signals (i.e., brain and body) (Fig.1A). This perspective highlights the need to understand cognition from an embodied standpoint, as the level of cognitive activity (e.g., level of intent) involves signals from both CNS and PNS.

However, much of the research on cognition focuses solely on the deliberate component of behaviors. Although there are merits in exploring this subset of behaviors, neglecting to consider a wider scope of movements may result in an incomplete view of the human nervous system. For instance, behaviors that occur automatically/spontaneously beneath the awareness are known to aid in the fluidity of movements by supporting the deliberate segments of behaviors [4, 14, 15]. The variability contained in these types of motions are informative in characterizing an individual's disposition and pathological condition [16], and have helped design personalized interventions in autism [17]. Indeed, recent research suggests that there is a wealth of information in the spontaneous behaviors that are commonly discarded or simply neglected in many cognitive neuroscience studies [18], and these studies instead rely on tasks that use discrete data (e.g., obtained from mouse clicks or pencil-and-paper means) to quantify unambiguous aspects of behavior. These methods describe conscious motor processes at the expense of discarding processes that occur largely beneath the awareness. The latter are in fact the bulk of what comprise human behaviors. Studying these

automatic/spontaneous segments are bound to fill a large gap of our knowledge base and are likely to reshape the way we think the brain works.

1.4. Cognitive Load under SPIBA

In this thesis, we attempt to characterize different levels of cognitive load with an embodied approach. Given the closed loop nature of the brain-body interactive control, it may be possible to explicitly vary the level of cognitive load an individual is exposed to, and examine the consequent patterns of variability in the underlying biophysical signals. Indeed, because the level of intent can be reflected in the statistics of an individual's movement fluctuations (explained more in detail in section 2.4.3) we may be able to characterize the level of cognitive load through the movement statistics.

In order to characterize cognitive load from the signals obtained from different layers of the nervous systems, we intend to employ a new statistical platform for the individualized behavioral analyses (SPIBA) [19]. Deployed by Torres's research team, SPIBA enables characterizing the variability in multi-sensory-motor signals under a common unifying scale, as the individual performs natural movements. More specifically, the new methods track minute fluctuations in the amplitude and timing of waveforms derived from the biophysical rhythms during natural movements that span across varying levels of intent, ranging from those that are voluntary to those that are autonomic. By adopting well-known statistical techniques and adapting them to the analyses of human biorhythms, we are able to track the participant's cognitive behaviors and decisions, and further obtain a glimpse of the afferent feedback the brain may receive during natural movements.

Employing the SPIBA on biophysical signals gathered under different levels of cognitive load can potentially be an objective, novel, and a robust way to comprehensively characterize cognitive loads across different layers of the nervous systems, and would help guide research in the field of embodied cognition. Cognitive load can be considered a multidimensional construct, where the load represents how a certain task may be imposing on the ongoing cognitive processes [20]. Most cognitive studies that attempt to measure cognitive load do so via post-hoc subjective assessments [20-22]. There is a paucity of studies that have objectively assessed cognitive load by examining the continuous psycho-physiological changes under different levels of cognitive load. The extant literature on this subject reports the use of eye movement signals, eye blink intervals, heart rate and heart rate variability, galvanic skin response, and brainwave signals [23-27]. However, these studies often show differing results among each other, presumably due to the type of tasks they tested. Indeed, there are multiple dimensions in cognitive capacities, so different tasks may result in different changes of the physiological signals. Also, if the physiological waveforms are examined under disparate scales without considering the heterogeneity of the human phenotypes, the results will be difficult to interpret and generalize. Moreover, the analytics of these studies oftentimes assume a priori a theoretical normal distribution without empirically testing the validity of such assumption across the population at large. This is such a common practice that paradigms such as the significant hypothesis testing (see proposed alternatives here [28]) lead to the infamous p-hacking issues Psychology as a field faces today (see for example [29-31]). The indiscriminate use of parametric models and linear methods in data generated by complex systems with non-linear dynamics also casts doubt on many of the claims thus far assessed by these studies, and

the imposition of such assumptions tends to mask the data variability as noise, thus ignoring a wealth of physiological signals contained in the data. Lastly, these studies assess signals harnessed from one aspect of the nervous systems and study their variations in isolation, without assessing the interdependencies among the signals from different layers of the nervous system. All these aspects of the current paradigms contribute to the general confusion or contradictory results of these studies, and thus call for more robust and standardized metrics of physiological signals to objectively characterize the effects of cognitive loads on the interactions across different layers and processes of the nervous systems (**Fig.1A**). Here, we start by relaxing some of the theoretical assumptions on normality, linearity, and stationarity to systematically test the variability inherently present in the empirical data harnessed in tandem from multiple processes and layers of the CNS, the PNS and the ANS, as the person physically executes tasks with varying levels of cognitive load.

1.5. Our Goal

In this thesis, we examine the moment-by-moment minute fluctuations in the motor and heart signals of an individual under different levels of cognitive load, and address the possibility of interdependencies within the nervous systems by examining the three processes – deliberate, spontaneous, and inevitable. If cognitive activities impact signals across the closed feedback loop of different nervous systems due to the interdependencies of these signals, we expect to see shifts in the signals' statistics obtained from the three processes under different levels of cognitive loads. However, if cognitive activities do not impact signals that occur largely beneath the awareness (e.g., heart signals from inevitable processes), we may not see any statistical shifts in those signals under different cognitive load levels.

It should be noted that for this study, we apply a novel platform SPIBA to analyze the physiological signals with varying levels of control (ranging from voluntary, automatic to autonomic levels) in different processes (deliberate, spontaneous and inevitable). Under the SPIBA framework, we do not make a priori assumptions of normality or linearity in the data, and empirically characterize the stochastic signatures of the variability of movement kinematics in tandem with the underlying heartbeat variability. We estimate the continuous family of probability distributions most likely fitting the motion/heart data, acquired in tandem under explicitly manipulated levels of cognitive load conditions.

2. Materials and methods

2.1. Participants

Nine undergraduate students (2 males and 7 females) between the ages 18 and 22 were recruited from the Rutgers human subject pool system, and received credit for their participation. Participants provided informed consent, which was approved by the Rutgers University Institutional Review Board. Two participants were left-handed, and all had normal or corrected-to-normal vision.

During the experiment, the motor and heart signals were recorded for each participant. However, one participant's heart signals did not record successfully due to instrumentation malfunctioning, resulting in an analysis on motor data for nine individuals and heart data for eight individuals.

2.2. Sensor Devices

In this study, two sensor devices – motion capture system and a wireless heart rate monitor – were used to record the signals coming from the motion and the heart.

2.2.1. Motion capture

15 electromagnetic sensors at a sampling frequency of 240 Hz (Polhemus Liberty, Colchester, VT) were used to capture the participant's continuous motion. Nine sensors were placed on the following body segments using sports bands to optimize unrestricted movement of the body: center of the forehead, thoracic vertebrate T7, right and left scapula, right and left upper arm, right and left forearm, the dominant hand's index finger. An additional sensor was used to

digitize the body in constructing a biomechanical model using the Motion Monitor (Innovative Sports Training Inc., Chicago, IL) software. Among the remaining sensors, one was placed at the backside center of the iPad (Apple, Cupertino CA) display screen, which the participant was interacting with during the experiment, and four sensors were placed at the four corners of the table, on which the iPad was standing. During the experiment, the participant's motion was captured in real-time, recording the location and speed of the upper body movement.

2.2.2. Heart rate monitor

Heart signals were obtained via electrocardiogram (ECG) from a wireless Nexus-10 device (Mind Media BV, The Netherlands) and Nexus 10 software Biotrace (Version 2015B) at a sampling rate of 256Hz. Three electrodes were placed on the chest according to the standardized lead II method, and were attached with adhesive tape. A typical ECG data includes a set of QRS complexes, and detecting R-peaks (within the QRS complex) is essential, as the heart rate metrics needed for this study focuses on the oscillation of intervals between consecutive heartbeats. In order to remove any baseline wandering and to accurately detect the R-peaks, ECG data were preprocessed using the Butterworth IIR band pass filter for 5-30Hz at 2nd order. The range of the band pass filter was selected based on the finding that a QRS complex is present in the frequency range of 5-30Hz [32]. To retrieve the time between R-peaks (i.e., inter-beat intervals, IBI) from the preprocessed ECG data, simple peak detection method was used, and was plotted using Matlab graphics to ensure that there were no missed R-peaks.

2.3. Stimulus apparatus and experimental procedure

Once all sensors were donned and calibrated, participants were seated at a table facing an iPad used as a touchscreen display. An in-house developed MATLAB (Release 2015b, The MathWorks, Inc., Natick, Massachusetts, United States) program controlled the presentation displayed on the touchscreen display, and also recorded the timing and location of the touches made by the participant. The MATLAB program was presented on the touchscreen display using the TeamViewer (Germany) application.

As shown in **Fig. 2**, for each trial, the participant was presented with a circle on the center of the display screen. This presentation prompted the participant to touch the circle on the screen within five seconds. Subsequent to the touch, the participant heard a tone at 1000Hz for 100ms. The duration between the touch and the tone was randomly set to be 100ms, 400ms, or 700ms. Then, on the display screen, the participant was presented with a sliding scale ranging from 0 to 1. On the sliding scale, the participant indicated how long they perceived the time to have elapsed between the touch and the tone, by touching the corresponding number on the scale within five seconds. Note, the five seconds time window allowed ample time for the participant to touch the screen at their own pace, as the time to reach the screen and then to retract the hand took approximately 1.5s. **Table A1** summarizes the median time to move the hand under each condition. The experiment consisted of three conditions – control, low-cognitive-load, and high-cognitive-load condition. Under the control condition, the participant simply performed this task for 60 trials. Under the low-cognitive-load condition, the participant performed these tasks for 60 trials, while repeatedly counting out loud one through five. Under the high-cognitive-load condition, the participant performed

these tasks for 60 trials, while counting backwards from 400 subtracting by 3. For both low- and high-cognitive-load conditions, the participant was instructed to count at a pace that was most comfortable to oneself. Participants took breaks in between conditions, and the entire experiment took about 40 minutes.

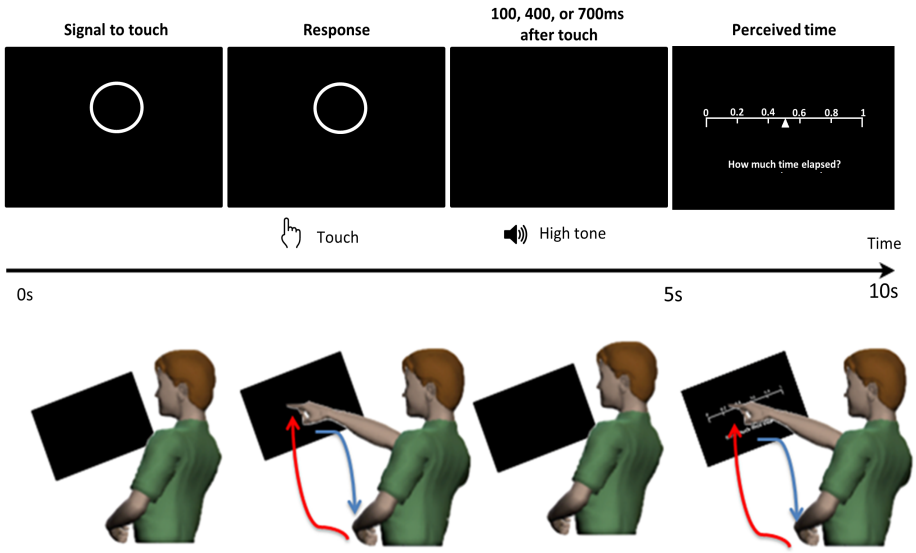

Figure 2. Experimental design. The participant was presented with a display screen as shown in the top panel. During the first five seconds, the screen presented a circle prompting the participant to touch the circle on the screen. After the touch, the participant heard a tone. The duration between the touch and the tone was randomly set to be 100ms, 400ms, or 700ms. In the next five seconds, the participant was presented with a sliding scale, where the participant would indicate how long they perceived the time to have elapsed between the touch and the tone, by touching the corresponding the number on the scale. For each trial, the participant made a pointing gesture to touch the circle and to indicate their time estimation on the sliding scale. The pointing movement is composed of a goal-directed segment (red) and a spontaneous segment (blue) as shown in the bottom panel.

2.4. Data analysis

2.4.1. The Statistical Platform for Individualized Behavioral Analyses (SPIBA)

The current study employs a new platform, SPIBA [19], which was created for personalized assessments required in the Precision Medicine and mobile Health concepts [33] (**Fig. 3**). For this study, the SPIBA was used to first characterize each participant individually, which could potentially be used to identify groups based on their similar statistical patterns in subsequent

studies. This platform stands in stark contrast to current approaches in science (e.g., significant hypothesis testing method), which compare groups that are assumed to follow a Gaussian distribution with homogenous variance. The pitfalls of such methods have been discussed by others [28, 34] and the Bayesian framework was offered as an alternative to address some of the known weaknesses. However, the Bayesian approach has not been adapted to analyze multiple types of biophysical data obtained from different layers of the nervous systems.

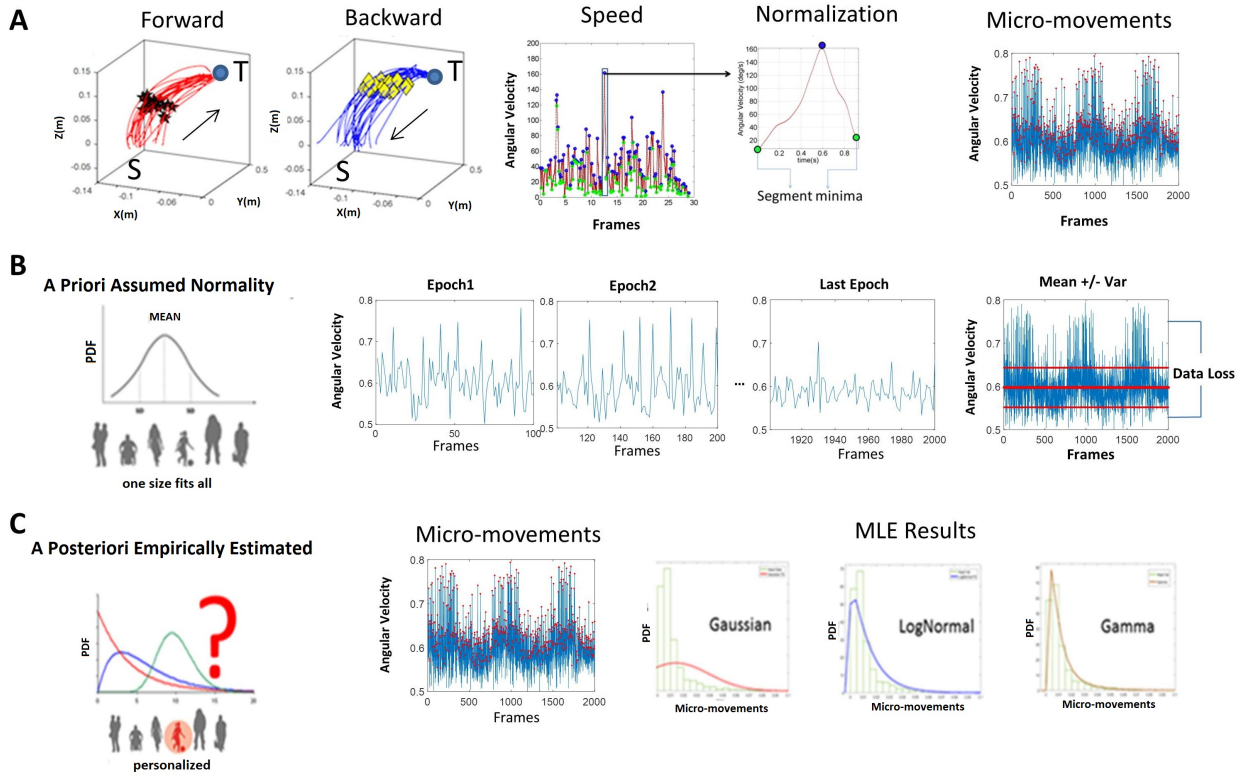

Figure 3. Comparison between traditional analytics and a personalized statistical approach (Statistical Platform for the Individualized Analyses of Behavior - SPIBA) used in the current study (A) Raw kinematic signals are obtained from motion trajectories during forward goal-directed (red) and backward spontaneous (blue) movements. "S" indicates the starting location of the hand, "T" indicates the target location, and arrows indicate the flow of the motion. Based on the positional trajectories as such, velocity-dependent metrics are obtained and converted to speed temporal profiles; then the fluctuations in the amplitudes of peaks are obtained and normalized to range between 0 and 1. These are the micro-movement waveforms extracted from any nervous systems - in this case, hand kinematics. **(B)** Traditional models assume that the data follows a priori Gaussian random process with additive statistics. As such, the assumed theoretical Gaussian moments (e.g., the mean and the variance) are used to analyze data, by averaging the waveform's peaks across a pre-set number of frames. Typically, pre-selected epochs would be averaged to determine the Gaussian mean, and fluctuations beyond a standard deviation from the Gaussian mean (denoted by the red lines) would be smoothed out as "noise" resulting in data loss. The assumed standard deviation would simply be the average of that "noise". This is the traditional ***"one-size-fits-all"*** approach that is applied in the data analysis of health and brain sciences today. **(C)** The same micro-movements waveform is analyzed using SPIBA. SPIBA does

not assume *a priori* any theoretical distribution. Instead, it accumulates events until the estimation process yields tight confidence intervals to fit various families of probability distribution functions. In this case, the Gaussian distribution, the lognormal distribution, and the Gamma distribution are used to illustrate the process of finding the best fitting distribution to characterize the data. Maximum likelihood estimation was used with a 95% confidence interval criterion to determine the best fitting distribution. We will later show that micro-movements generally follow a continuous Gamma process, and that the noise-to-signal ratio of these micro-movements are of interest in the SPIBA framework.

The SPIBA framework, with the use of a new data type coined *"the micro-movements"* of biophysical signals (explained in the following section 2.4.2.), was precisely designed to longitudinally tackle the emergence, dynamic development, maintenance and degeneration of the signals generated by the multi-layered nervous systems, including those with different pathologies over the human lifespan [16].

2.4.2. Definition of micro-movements

The raw biophysical data continuously registered from physiological sensors (i.e., physiological signals obtained from brain waves (EEG), heart activities (ECG), respiration patterns, kinematics from bodily, head and eye movements, tremor data, etc.) give rise to a time series of peaks and valleys, which varies in amplitude and timing (**Fig. 4**). The fluctuations in amplitude and timing of the peaks are assumed to characterize a continuous random process where events in the past may (or may not) accumulate evidence towards prediction of future events. These fluctuations (e.g., peak amplitude, inter-peak intervals) are the "*the micro-movements*" of biophysical signals.

The micro-movement waveforms derived from the time series of biophysical signals are used to represent a continuous random process under the general rubric of Poison Random Process. To be more precise, we examine the kinematic/physiological signals and detect the peaks, and consider them random amplitudes and random times. To model them, we build on

our original work [6] whereby the amplitudes and inter-peak intervals are modeled as independent and identically distributed (I.I.D.) random variables following a Gamma distribution (rationale behind this is explained in section 2.4.4).

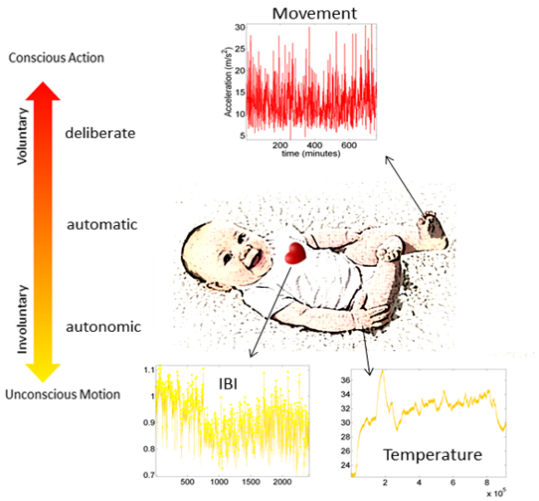

Figure 4. Micro-movements from different nervous systems' biorhythms (e.g., heart activity, temperature, and movement) registered from physiological sensors. Raw biophysical signals give rise to a time series of peaks and valleys, which vary in amplitude and timing. The fluctuations in the amplitude and timing of the peaks are the 'micro-movements' of biophysical signals.

In the current study, we show an example of using SPIBA and micro-movement data involving signals harnessed in tandem from the CNS, PNS and ANS. To that end, we will examine biophysical data from body movements and the heart of an individual exposed to a decision-making task with different levels of cognitive load.

2.4.3. Different Classes of Movement Segments - Forward versus backward

For this study, the continuous trajectory of the participant's dominant hand index finger was decomposed into forward and backward movements (**Fig. 2**). The forward movement corresponds to the movement when the hand resting at the table would reach out to touch the display screen. As this movement involves an explicit goal in mind (i.e., to touch the display

screen), this movement involves a high level of intention. On the other hand, the backward movement corresponds to the movement when the hand touching the display screen would spontaneously (without any instruction) retract back to the table. Because this uninstructed movement does not involve an explicit goal and is more automatic, it involves a relatively lower level of intention. The heart inevitably beats throughout both motions, and as such, provides a third type of process to follow in tandem with the action.

For each trial, as the participant moved the dominant hand from the table to the display screen and back to the table, the movement trajectory consisted of forward and backward movements. The two types of movements were separated for each trial, by identifying the time when the distance of the sensor locations between the index finger and the display screen was at the minimum. Naturally, at this time point, the linear velocity of the index finger reaches near instantaneous zero (see **Fig. A1-A**). Hence, the forward movement would correspond to the movement from the time when the index finger is resting on the table until the time the finger stops at the display screen. The backward movement, on the other hand, would correspond to the movement from the time when the index finger stops at the display screen until it reaches back to the table and rests (i.e., the speed value is near zero again).

The rationale behind the separation between forward and backward movement is that one is instructed and goal-directed while the other is not. As such, their levels of intent differ, and the statistical characteristics have been shown to differ between forward and backward movements (i.e., motion segment with high versus low level of intent) during reaching, pointing, and grasping actions among different patient populations and across the general

human population [6, 9, 11, 14, 35]. For that reason, we expect that separating the movements in such a manner would allow us to examine the impact of cognitive load on movements involving different levels of intent.

Analyses of the sensors from other body parts are beyond the scope of this paper, as signals obtained from those parts involve different levels of control, and therefore different processes from those obtained from the dominant hand's index finger (i.e., end effector). For that reason, analysis of the signals obtained from other parts of the other body will be disseminated in future work.

2.4.4. Micro-Movements Analytics for Motor Signals

For each forward and backward movement, we examined the linear and angular positional data and their higher order derivatives: linear velocity, angular velocity, linear acceleration, angular acceleration (**Fig. A1**). For each, peak data (e.g., peak amplitudes, inter-peak intervals) were identified, converted to micro-movements (see below) and gathered across all trials. Among the four types of parameters, for both forward and backward movements, angular acceleration was analyzed, as it showed to have the largest number of peaks.

The current paradigm relies on the statistical power of an estimation procedure (which will be detailed in the next paragraph) so the higher the number of samples used to make an estimation, the less taxing the experiment is to the participant, as it takes less time to attain a robust estimate. For instance, during a typical point-to-point reaching action, which consists of a single forward and backward movement, the linear velocity would typically provide two samples of peak data– one for forward and one for backward movement. In order to gain

enough peak data from the linear velocity speed profile during a single experimental session, the participant would need to perform at least 100 reaches, which would lead to fatigue-related effects. Instead, using data that produces the largest number of peak data would result in shorter experiments, allowing us to include other conditions. For that reason, the current study focused on examining the peak data obtained from angular acceleration, as this would provide the most power in the statistics with the shortest time.

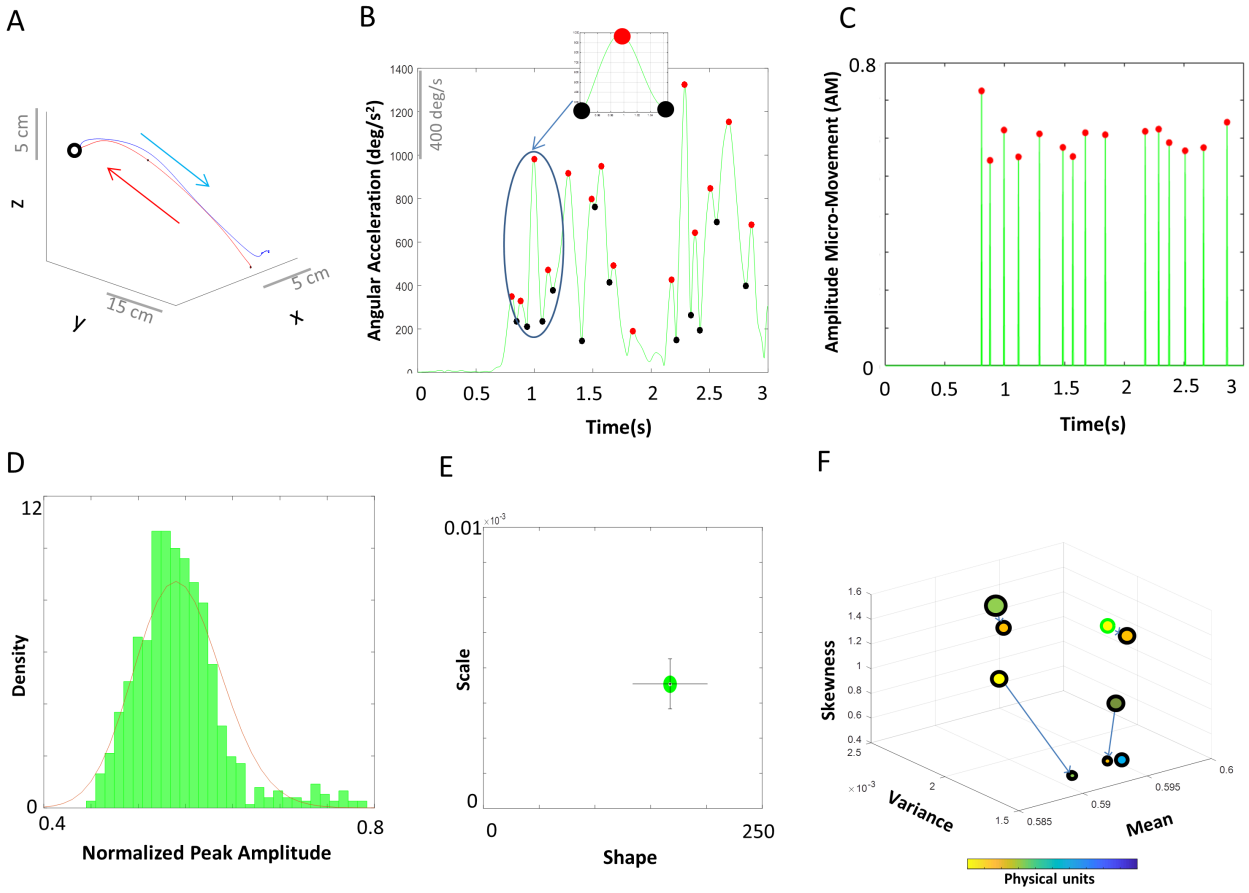

Figure 5. Analytical and Visualization Methods (A) A typical trajectory of the dominant hand performing a single pointing movement. The movement trajectory was separated by forward (red) and backward segments (blue), where the forward movement corresponds to the movement from the time when the index finger is resting on the table until the time the finger stops at the target display screen. The backward movement corresponds to the movement from the time the index finger stops at the display screen until the time it reaches back to the table. **(B)** Time series of angular acceleration of the dominant hand's index finger during a typical pointing task. Peaks (maxima) and valleys (minima) are shown in red and black dots, respectively. The inset shows a zoomed-in picture of a single angular acceleration segment (i.e., two local minima and a single peak in between). This is a schematic of computing the AM (normalized peak amplitude) from a continuous time series of signal data, where the AM is computed by dividing the peak value by the sum of the peak value and the average of the signal values

between the two local minima. **(C)** Peak train for a typical pointing task. All peak values from 'B' are normalized between 0 and 1, while all non-peak values are set to 0. **(D)** All AMs values were identified and gathered across all trials. For these peak data, a frequency histogram was then plotted, and fitted with a Gamma probability distribution function using maximum likelihood estimation. In addition to the AM values, we can also plot the histogram of TM values, and proceed to the next step. **(E)** The estimated Gamma parameters from the fitted probability distribution were then plotted on a Gamma parameter plane, with lines representing the 95% confidence interval. **(F)** Empirically estimated mean, variance, and skewness of the fitted Gamma PDFs were plotted on the x, y, and z axes respectively. The size of the marker reflects the level of kurtosis, where larger size indicates high kurtosis level of the fitted PDF. The arrows connecting the markers indicate the order of the task conditions. The marker's face color represents the median values of the underlying physical unit. The marker with green edge color corresponds to the instance of estimated distribution described in 'D' and 'E', and markers with black edge color are shown to illustrate other instances of estimated distributions.

In analyzing the peak data, peak amplitudes and inter-peak intervals were examined. First, to avoid allometric effects [36] due to different anatomical sizes across different participants, peak amplitude data were normalized. Normalized peak amplitude (coined *amplitude micro-movements 'AM')* was thus computed by dividing the peak angular acceleration by the sum of the peak angular acceleration and the average angular acceleration between the two local minima (**Fig. 5B**). Generally, higher average values result in lower normalized peak amplitude values. Likewise, shifts towards higher values of this index indicate lower average values.

$$\textit{Normalized peak amplitude (AM)} = \frac{Peak\ Amplitude}{(Peak\ amplitude + Average\ of\ Signals\ within\ a\ single\ segment\ )}$$

Inter-peak interval (coined *timing micro-movement 'TM')* index was computed by extracting the time elapsed between consecutive peaks. These two types of peak data (AM, TM) can be visualized in a peak train as shown in **Fig. 5C**.

The two types of peak data were then accumulated across all trials for each condition, and a frequency histogram was plotted using optimal binning [37, 38] (**Fig. 5D**). The histogram

was then fitted using maximum likelihood estimation (MLE) to estimate the best continuous family of probability distributions that fit the data.

Prior work from our lab had explored the differences between multiplicative (e.g., lognormal family) and additive (e.g., exponential families) random processes of the micro-movement data on motor signals extracted from voluntary, automatic, and involuntary motions across thousands of participants. Among these are micro-movements data from boxing routines involving voluntary and spontaneously performed movements [4, 5], forward-retracting loops during target directed reaches [6, 9, 11, 14, 35], natural walking involving automatic gait patterns [39], and involuntary head motions during resting state within fMRI experiments [18]. In all cases, the continuous Gamma family of probability distributions has been the best fit (based on MLE and Kolmogorov-Smirnov tests for empirically derived cumulative distributions), since these data would widely range from the exponential to the normal distribution. As such, the human motion data across different levels of control (e.g., high level of voluntary control and low level of autonomic control) seem to be well characterized by the Gamma family of distributions (which is inclusive of exponential and normal distributions), reflecting additive random processes in continuous physiological data during natural states of behavior.

As in other studies of motor behavior [4], here we found the lognormal distribution as a good fit for the motor data. However, given that the difference in the goodness of fit is small relative to that for the Gamma estimates, and that exponential distributions are best fit in the motor data of pathological cases (not included in this thesis) [5, 6] we opted for the Gamma

family. This family encompasses a wider range of distributions (e.g., normal, skewed, exponential), allowing us to utilize a unifying family of distributions across different physiological signals and across different population (**Fig. A2**). For that reason, we used the micro-movements of motor data as input to a continuous Gamma process.

From the Gamma probability distribution function (PDF), the two parameters – shape (a) and scale (b) - were estimated for each histogram of the micro-movement data, using MLE with 95% confidence intervals (CI). The estimated parameters with their CI were plotted on a Gamma parameter plane, where the x-axis represents the shape parameter value and y-axis represents the scale parameter value (**Fig. 5E**). This plot would allow us to interpret the level of noise and regularity inherent in the biophysical signal. This point is further elaborated in the subsequent section 2.4.5. Additionally, the estimated Gamma PDF was visualized by computing the PDF moments and plotting them in a four-dimensional graph (**Fig. 5F**). Here, the empirically estimated mean, variance, and skewness of the fitted Gamma PDFs were plotted on the x, y, and z axes respectively. The size of the marker reflects the level of kurtosis, where larger size indicates higher kurtosis level (distributions with sharper peaks) of the fitted PDF and a zero skewness values indicates a symmetric distribution. This graph would allow us to visualize the statistical features, and understand how the stochastic signatures shift across different conditions or individuals. The arrows were included to indicate the orderly flow of change across different conditions. Note, since we scale the peak amplitude values along a unit-less range from 0 to 1 to represent AM, for the 4D graph of AM Gamma moments, we also included the actual physical ranges of the data underlying the AM (expressed in deg/s^2.) To that end, we

color the marker's face to represent the median of the physical values, and the marker's edge to represent the condition (i.e., cognitive load type).

2.4.5. Stochastic signatures of micro-movements

It is noteworthy that the statistics of an individual's micro-movements (i.e., fitted shape and scale parameters of the estimated Gamma PDF) reflect the individual's features within a given context along with the individual's level of intent. In fact, the quantification of how these individual's fitted parameters shift on the Gamma parameter plane (e.g., location, frequency/magnitude in shifts across time) across contexts are unique to each individual, and thus have been referred to as the 'stochastic signatures' [6, 16].

Within the Gamma family of distributions, the estimated PDFs from human motions plotted on the Gamma parameter plane have a characteristic range: along the shape (horizontal) axis the empirically estimated values range from the memory-less exponential distribution (where the shape parameter is 1) to the symmetric Gaussian-like distribution (where the shape parameter is high), with skewed distributions in between. Along the scale (vertical) axis the empirically estimated values represent the level of variability of the distribution, from low to high dispersion levels.

In general, stochastic signatures of healthy adults, particularly skilled athletes, tend to exhibit a higher shape and lower scale parameter values (i.e., follow a Gaussian-like distribution) [4, 5], while individuals with compromised systems concerning pathologies such as Autism spectrum disorder, schizophrenia, Parkinson's disease, etc. or injury due to stroke or

coma states, tend to exhibit a lower shape and higher scale parameter values (i.e., statistical signatures closer to exponential distribution) [6, 11, 14, 16, 35].

Furthermore, when an individual's movement involves a higher level of intent (e.g., forward movements such as pointing at a target), the statistics tend to exhibit a higher shape and lower scale parameter values, while those involving a lower level of intent (e.g., backward movement such as retracting the hand) tend to exhibit a broader range of shape and scale parameter values [4]. It is worth mentioning that the noise-to-signal ratio (NSR, otherwise known as the Fano Factor [40]) in a Gamma PDF is equivalent to the scale parameter value. Hence, as the scale value increases so does the NSR. Interestingly, it has been found that during repeated motor performance, fatigue contributes to the micro-movements of motor signals by exhibiting higher NSR in the statistics, as the dispersion of the empirically estimated distribution broadens [41, 42].

2.4.6. Micro-Movements Analytics for Heart Signals (inter-beat interval)

Similar to the analysis performed on the micro-movement peak data of motor signals (i.e., AM, TM), we applied the distributional analyses on the IBI data for each condition. As with the hand kinematics, we fitted the PDF using MLE. Histograms for the IBI data were fitted among the Gamma, exponential, lognormal, and normal for each condition, and we determined that the Gamma family of distribution would be appropriate for fitting the IBI data (**Fig. A3**). For that reason, the parameters of the Gamma PDF were estimated for each histogram of the IBI data, and the shape and scale values were plotted on the Gamma parameter plane with 95% confidence intervals.

3. Results

3.1. Low Cognitive Load *vs*. High Cognitive Load

3.1.1. Deliberate *vs.* Spontaneous Processes: CNS Assessment of Voluntary and Automatic Control of Hand Kinematics

The estimated Gamma parameters of motor signals' micro-movement peak data were first compared between the two conditions – low cognitive load and high cognitive load. These micro-movements were extracted from segments of pointing gestures, when the participant merely reached the display screen to touch the circle. The shape and scale parameters of the continuous Gamma family of probability distributions with 95% confidence were plotted on the Gamma parameter plane, and compared between the two conditions for the following micro-movement data – AM and TM.

Goal-Directed (Forward) Segment For the forward movement, which involves a relatively high level of intent, the estimated Gamma parameters of the AM PDF did not show a distinct trend in the separation between the two conditions at 95% confidence interval (**Fig. A4-A, B**). Specifically, one participant showed distinct estimated Gamma parameters between the two conditions, such that movements under the low-cognitive-load condition showed a lower shape and higher scale parameter than movements under high-cognitive-load condition. However, the other eight participants did not show such a distinction between the two conditions. The estimated Gamma parameters of the TM PDF also did not show a distinct trend in the separation between the two conditions at 95% confidence interval (**Fig. A4-C, D**). Specifically, one participant showed distinct estimated Gamma parameters between the two

conditions, such that movement statistics under the low-cognitive-load condition had a higher shape and lower scale parameter than movement statistics under high-cognitive-load condition. However, other eight participants did not show such distinction between the two conditions. **Table A2** summarizes the p-values of the statistical comparisons across these two conditions for each participant using a non-parametric one-way ANOVA.

Spontaneous Retraction (Backward segment) For the backward movement, which involves a relatively low level of intent, the estimated Gamma parameters of the AM PDF did not show distinct separation between the two conditions at 95% confidence interval for all participants (**Fig. A5-A, B**). The estimated Gamma parameters of the TM PDF also did not show distinct separation between the two conditions at 95% confidence interval for all participants (**Fig. A5-C, D**).

Overall, the estimated Gamma parameters of the micro-movement peak data did not show any consistent pattern in distinguishing between movements under low-cognitive-load condition (i.e., dual task of counting forward) and high-cognitive-load condition (i.e., dual task of counting backwards) across all participants.

3.1.2. Inevitable Processes: ANS assessment of Autonomic Control of IBI

The estimated Gamma parameters of the heart's IBI data were compared between the two conditions. Similar to the analysis performed for the motor data, the shape and scale parameters of the IBI's estimated probability distributions with 95% confidence were plotted on the Gamma parameter plane, and compared between the two conditions.

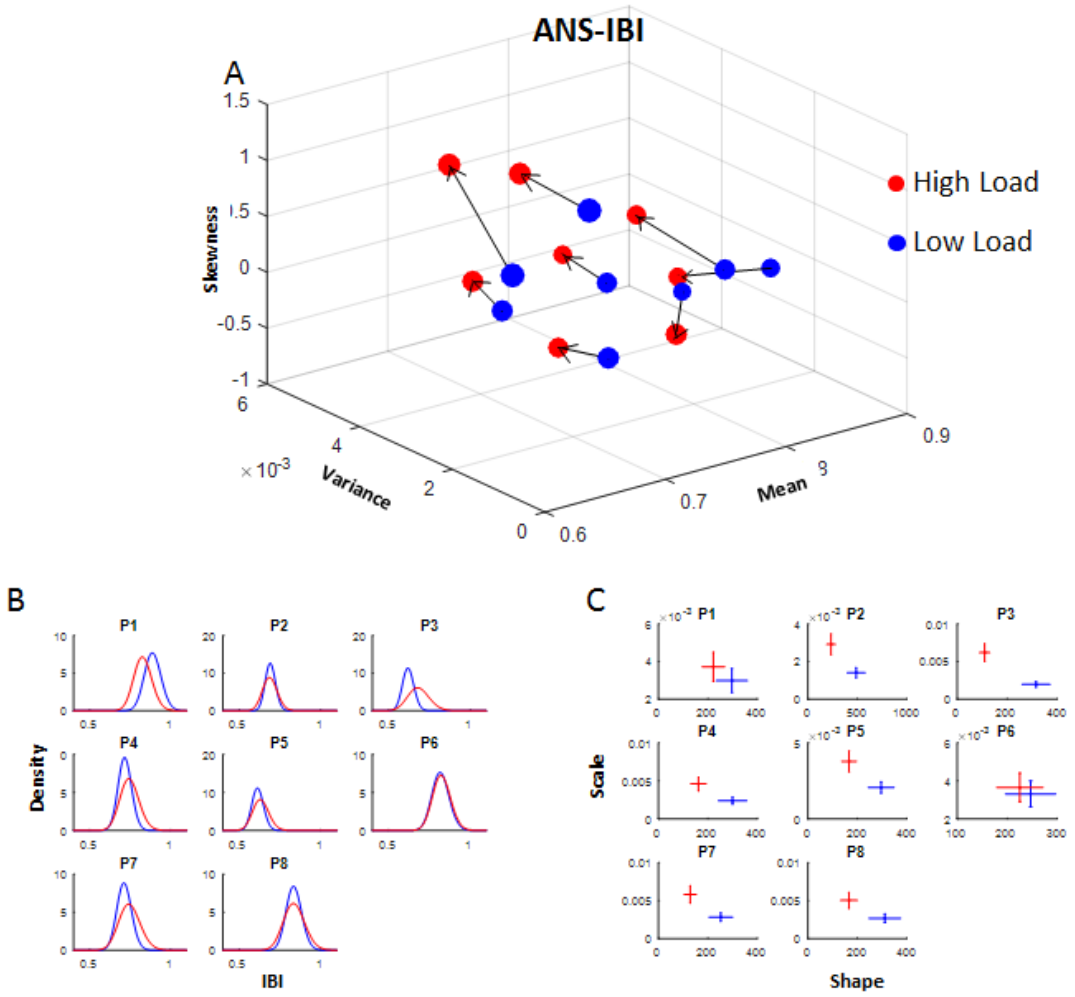

Figure 6. ANS autonomic control assessment under high- and low-cognitive-load conditions. IBI signal. **(A)** Estimated Gamma moments, **(B)** PDF, and **(C)** parameters of IBI for low-cognitive-load condition (blue) and high-cognitive-load condition (red) per participant (P1-P8). The estimated Gamma parameters of the IBI probability distribution function showed a distinct trend in the separation between the two conditions, such that IBIs under the low-cognitive-load condition showed a higher shape and lower scale parameter than IBIs under the high-cognitive-load condition.

Contrary to the hand kinematics data (AM and TM) from the forward and backward motions tapping into deliberate and spontaneous processes respectively, the estimated Gamma parameters characterizing the PDFs of the IBI showed a distinct trend in the separation between the two conditions at 95% confidence interval. Specifically, seven participants showed distinct estimated Gamma parameters between the two conditions, such that IBIs under the low-cognitive-load condition showed a higher shape and lower scale parameter than IBIs under

high-cognitive-load condition (**Fig. 6**). One participant did not show such distinct separation at 95% confidence interval, but exhibited a similar trend. **Fig. 6A** shows the individualized profiling of each participant's stochastic transitions from low to high-cognitive-load condition, with the arrow marking the order of those conditions. As the cognitive load increases, there is a tendency across participants (six out of eight participants) to increase the PDF skewness (note, the PDF is symmetrical when the skewness value is 0), and an overall tendency to increase the PDF variance.

The increase in the IBI's variance as the cognitive load increases is reflected in the increase of the noise-to-signal ratio (i.e., the value of the Gamma scale parameter) across all participants. On the other hand, there is no consistent trend in the mean IBI across participants when cognitive load increases, since the mean IBI is higher in some cases and lower in others. As such, the dispersion of the distribution is more informative as it systematically separates the performance between the two conditions for all participants.

Overall, the IBI's estimated PDF under the high-cognitive-load condition showed less symmetry (i.e., lower shape parameter value) and higher noise-to-signal ratio (i.e., higher scale parameter value) than under the low-cognitive-load condition. Based on our empirical evidence from other experiments, and the fact that a leftward shift along the shape axis on the Gamma parameter plane tends towards the limiting exponential case of the Gamma family, we infer that under high cognitive load, an individual's IBI tends to become noisier and less predictable. As such, we can see that the impact of higher cognitive load is funneled through the inevitable processes – characterized here through the IBI timing.

3.2. Pointing vs. Time estimation (decision making) task

To compare different levels of cognitive load, micro-movements of motor and IBI data were also compared between two different types of tasks – pointing and time estimation. Each trial lasted for 10 seconds – in the first five seconds, the participant performed a simple pointing task, where she simply pointed at the circle presented at the display screen; in the subsequent five seconds, the participant performed a time estimation task, where she made the same pointing gesture towards the display screen, but was thinking about the elapsed duration while deciding on inputting the response. Data corresponding to the pointing task (i.e., data from the first five seconds of each trial) were aggregated across all trials of each experimental condition (i.e., control, low-cognitive-load, and high-cognitive-load conditions). Data corresponding to the time estimation task (i.e., data from the latter five seconds *of each trial*) were also aggregated across all experimental conditions (i.e., control, low cognitive load, and high-cognitive-load conditions). The data from these two tasks were then compared, under the assumption that the pointing task would entail a lower level of cognitive load than the time estimation task. This is because while the participant makes the same reaching gesture towards the display screen with one's dominant hand for both tasks, the time estimation task involves an additional task of making decisions. Indeed, decision making entails higher order representations, retrieval of memories, and error estimation, all of which would require more thought.

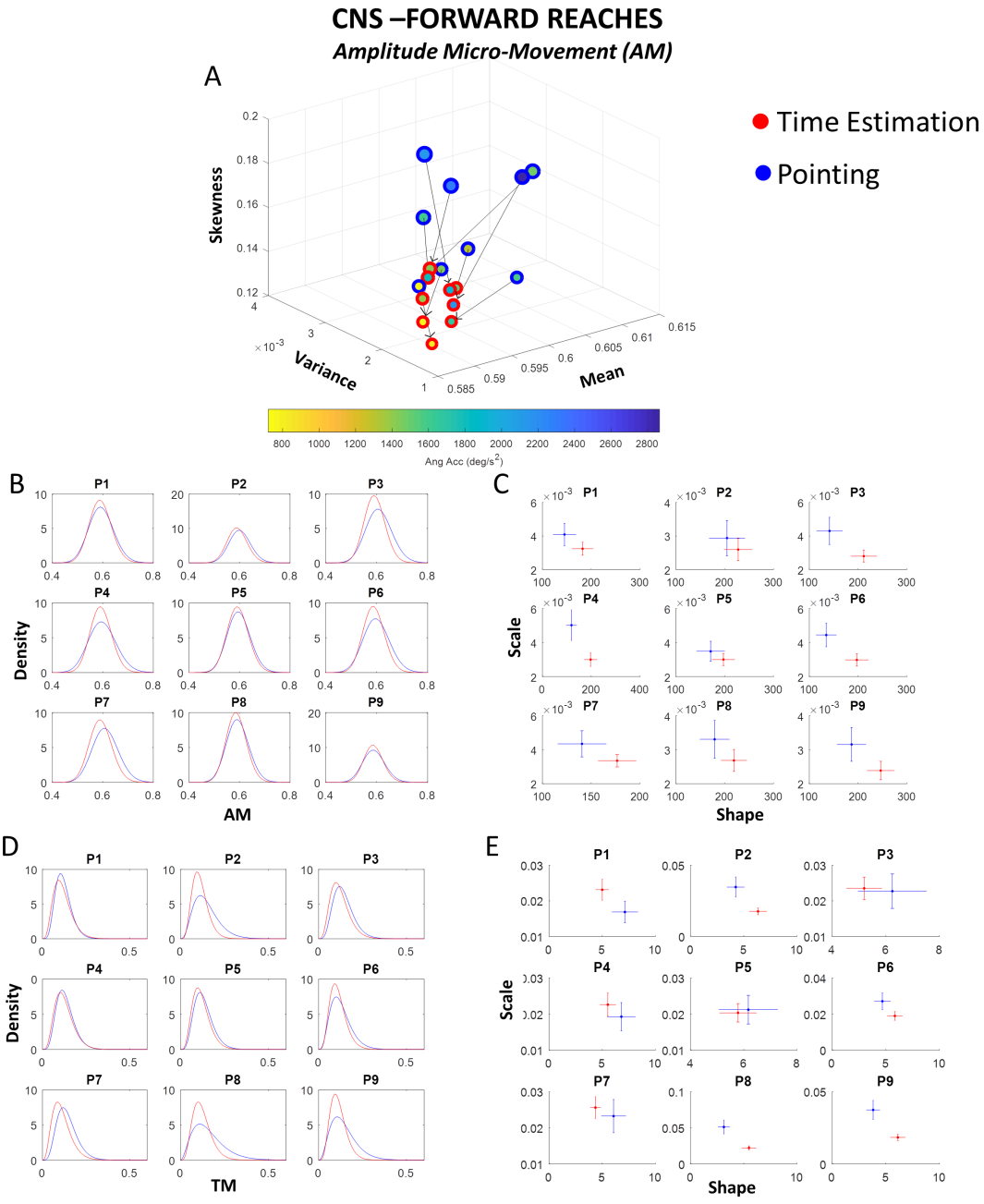

Figure 7. CNS voluntary control assessment of goal-directed forward movement during pointing and time estimation tasks. Kinematics signal of the hand for goal-directed forward segments. **(A)** Estimated Gamma moments, **(B)** PDF, and **(C)** parameters of the AM metric, and **(D)** estimated PDF and **(E)** parameters of the TM metric, for the pointing (blue) and time estimation task (red) per participant (P1-P9). The estimated Gamma parameters of the AM probability distribution function showed a trend in separation between the two tasks, such that the PDF during the pointing task entailed a lower shape and higher scale parameter than the PDF during the time estimation task. On the other hand, the estimated Gamma parameters of the TM PDF did not show a consistent pattern across all participants.

3.2.1. Deliberate and Spontaneous processes: CNS Assessment of Voluntary and Automatic Control of Hand Kinematics

Deliberate Processes – Voluntary (Forward) Segment For the forward movement, which involves a relatively high level of intent, the estimated Gamma parameters of the AM PDF showed a separation between the pointing and time estimation task at 95% confidence interval (**Fig. 7**). Specifically, on the Gamma parameter plane, for seven out of nine participants, movements during the pointing task showed a lower shape and higher scale parameter than movements during the time estimation task. Two participants did not show as much distinct separation at 95% confidence interval, but exhibited a similar trend. Further, when augmenting the parameter space to the four-dimensions (**Fig 7A),** we see that all participants show a major statistical transition across all moments. In particular, transitioning from pointing to time estimation task increased the speed of hand kinematics on average (lower AM suggests higher speed; see section 2.4.4), while the PDF became less variable with lower dispersion (NSR) level and more symmetrical in it shape. This result suggests that the statistics of the kinematics during time estimation tasks yield a very different outcome than those during pointing tasks, even though both involve a similar biomechanical structure. Specifically, the motor signals during the decision making task show to have better predictability in its signal than during a simple pointing task.

On the other hand, during the forward reaches, the estimated Gamma parameters of the TM PDF did not show a systematic pattern of distinct separation across all participants (**Fig. 7D-E**). Specifically, one participant's movement during the pointing task showed a higher shape and lower scale parameter than during a time estimation task. However, four participants

showed an opposite pattern, such that movement during the pointing task showed a lower shape and higher scale parameter than during a time estimation task. The rest of the participants' movement did not show separation between the two tasks at 95% confidence interval.

Spontaneous Processes – Automatic (Backward) segment For the backward movement, which involves a relatively low level of intent, as it was not instructed and had no explicit visual goal, the estimated Gamma parameters for the AM did not show separation between the pointing and time estimation task at 95% confidence interval for all participants (**Fig. 8D-E**). On the other hand, the estimated Gamma parameters of the TM PDF did show separation between the two tasks for all participants (**Figure 8B-C**). Specifically, for six participants, movement during the pointing task showed a lower shape and higher scale parameter than during the time estimation task at 95% confidence interval. The remaining three participants did not show as much distinct separation, but exhibited a similar trend as those six participants. The statistical effects are also reflected in the **Figure 8A** across all estimated Gamma moments, where estimating time (i.e., decision making) tends to systematically decrease the noise-to-signal ratio and the skewness of the distribution. Here, the timing is shorter (i.e., mean of TM are smaller), thus indicating a faster speed in the motion with lower variance (i.e., lower noise-to-signal ratio). As such, retractions made while making decisions are more focused than while retracting without making any decisions, since motions are executed in a fast manner with low noise while decisions are being made.

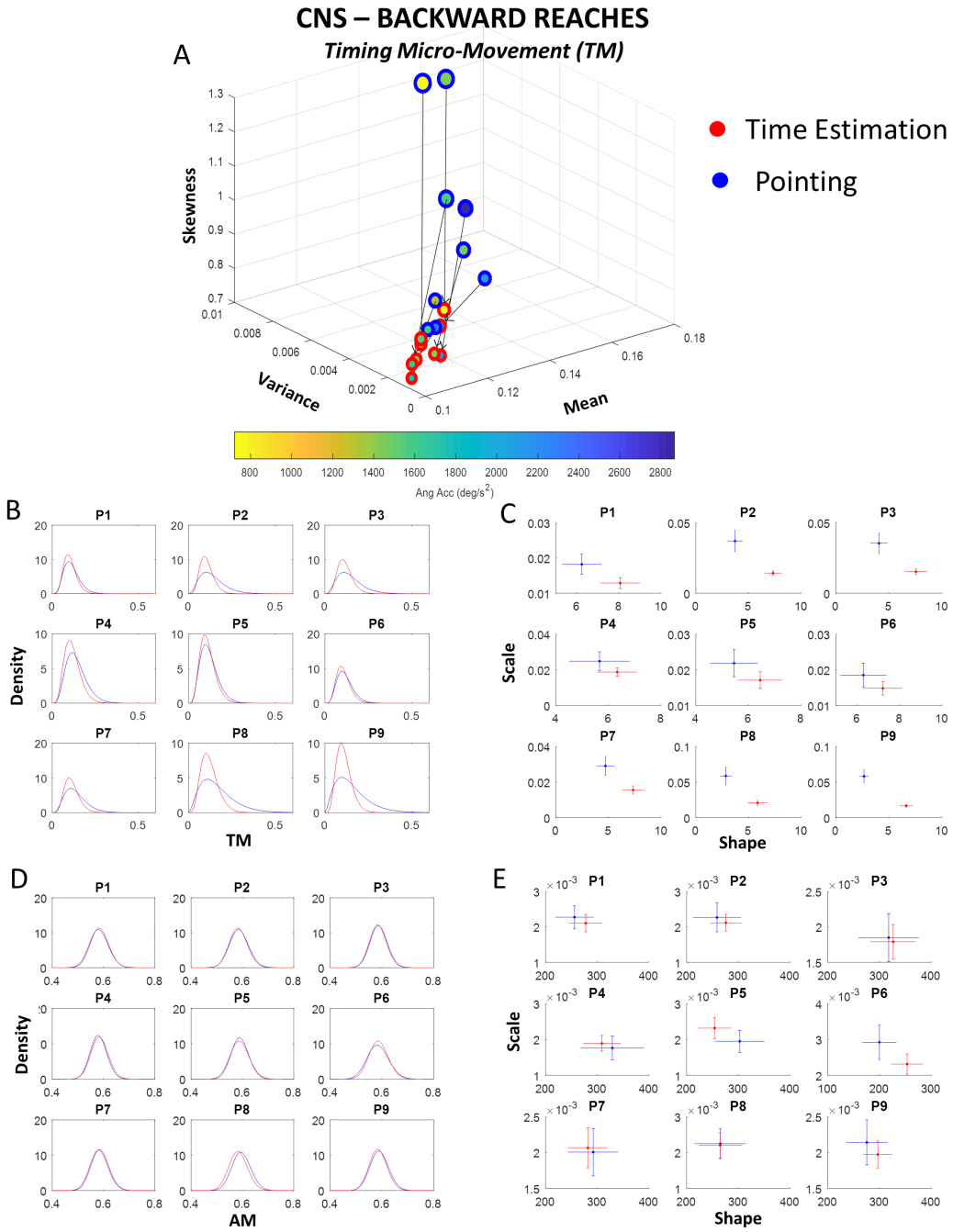

Figure 8. CNS automatic control assessment of spontaneous backward movement during pointing and time estimation tasks. Kinematics signal of the hand for spontaneous backward segments. **(A)** Estimated Gamma moments, **(B)** PDF, and **(C)** parameters of TM metric, and **(D)** estimated PDF and **(E)** parameters of the AM metric, for the pointing (blue) and time estimation task (red) per participant (P1-P9). The estimated Gamma parameters of the TM probability distribution function showed a trend in separation between the two tasks, such that the PDF during the pointing task entailed a lower shape and higher scale parameter than the PDF during the time estimation task. On the other hand, the estimated Gamma parameters of the AM PDF did not show a consistent pattern across all participants

Overall, different micro-movement metrics were shown to be informative in separating the two tasks –pointing and time estimation tasks - for the forward and backward movements. In differentiating the two tasks, if the movement entailed a higher level of intent (i.e., goal-directed forward movement), it was more informative to use the estimated Gamma parameters of the AM PDF, reflecting the moment-by-moment fluctuations in ***peak amplitude***. However, if the movement entailed a lower level of intent (i.e., spontaneous backward movement), it was more informative to use the estimated Gamma parameters of TM PDF, reflecting the fluctuations in the ***peak timing***. For both forward and backward movements, those involving a lower level of cognitive load (i.e., pointing task) exhibited a lower shape and higher scale parameter than movements involving a higher level of cognitive load (i.e., time estimation task). This implies that movements involving a higher level of cognitive load tend to exhibit a more predictable (i.e., higher shape parameter towards a symmetric Gaussian distribution) and less variable (i.e., lower dispersion registered in the scale parameter) statistical distribution.

3.2.2. Inevitable Process: ANS assessment of Autonomic Control using IBI

Contrary to the kinematics data (AM and TM), the estimated Gamma PDF parameters of the IBI did not show any separation between the pointing and time estimation task at 95% confidence interval for all participants (**Fig. A6-B**). In general, the estimated IBI PDF showed to be fairly similar for both tasks (**Fig. A6-A**).

4. Discussion

In this study, we were able to detect interdependencies between signals by examining the three processes – deliberate, spontaneous, and inevitable – using a new set of analytics and an experimental paradigm that probes the variability in the biophysical rhythms across multiple control levels of the nervous systems, as participants were exposed to different levels of cognitive load. These interdependencies were examined from the various motor and heart signals harnessed in tandem.

We were able to capture the effect of cognitive load at the voluntary, automatic/spontaneous, and autonomic control levels (i.e., from deliberate, spontaneous, and inevitable processes) and identified parameters characterizing cognitive load through the stochastic shifts of biophysical signals. Specifically, using a personalized method of statistical analysis, we detected the effects of cognitive load on the somatic-motor parameters, by contrasting signals obtained during basic pointing and pointing to indicate a decision on time estimation. Even though the underlying biomechanics of the pointing action was the same, we were able to quantify the interdependencies from deliberate and spontaneous processes, with more saliency in deliberate processes during goal-directed reaches through spatial parameters in the angular acceleration, where significant shifts in the stochastic signatures of the AM were quantified; and with more saliency in spontaneous processes during uninstructed hand retractions through temporal parameters of the angular acceleration, with stochastic shifts in the TM. We also identified the effects of cognitive load on the heart parameters, by contrasting signals obtained while participants counted forward and while they counted backwards. Here,

we were able to quantify the interdependencies from inevitable processes through the temporal parameters of the IBIs.

When we detected effects of cognitive load on the somatic-motor patterns (i.e., when contrasting a simple pointing task against a time estimation pointing task), we did not detect interdependencies from inevitable processes linked to the heart signals. Also, when we detected effects of cognitive load on the heart signals (contrasting a simple pointing task while counting backwards as opposed to counting forward), we found no effects on the stochastic signatures of the kinematics motor signal. This result implies that additional cognitive load can significantly change the physical states reflected in the motor kinematics without impacting the ANS signals, and that the ANS signals can also be affected by mental activity, even when the physical activity captured through the kinematics may show very subtle to no significant changes. In this sense we have demonstrated quantifying the interdependencies at different levels, spanning from the brain to the body to the heart. We next discuss the details of these results summarized in **Fig. 9**.

4.1. Cognitive load is reflected differently in motor and heart signals

Under the high-cognitive-load condition, where the participant was given a challenging dual task, the estimated Gamma PDF of IBIs showed to be more variable (i.e., higher scale parameter) and less predictable (i.e., lower shape parameter) than under the low-cognitive-load condition, where the participant was given an easier dual task. Although the estimated Gamma parameters of the IBI varied from subject to subject, there was a general trend to change signatures across all estimated moments (**Fig. 6A**). This suggests that the autonomic

heartbeat is affected by different cognitive loads in ways that are measurable using simple/existing instrumentation.

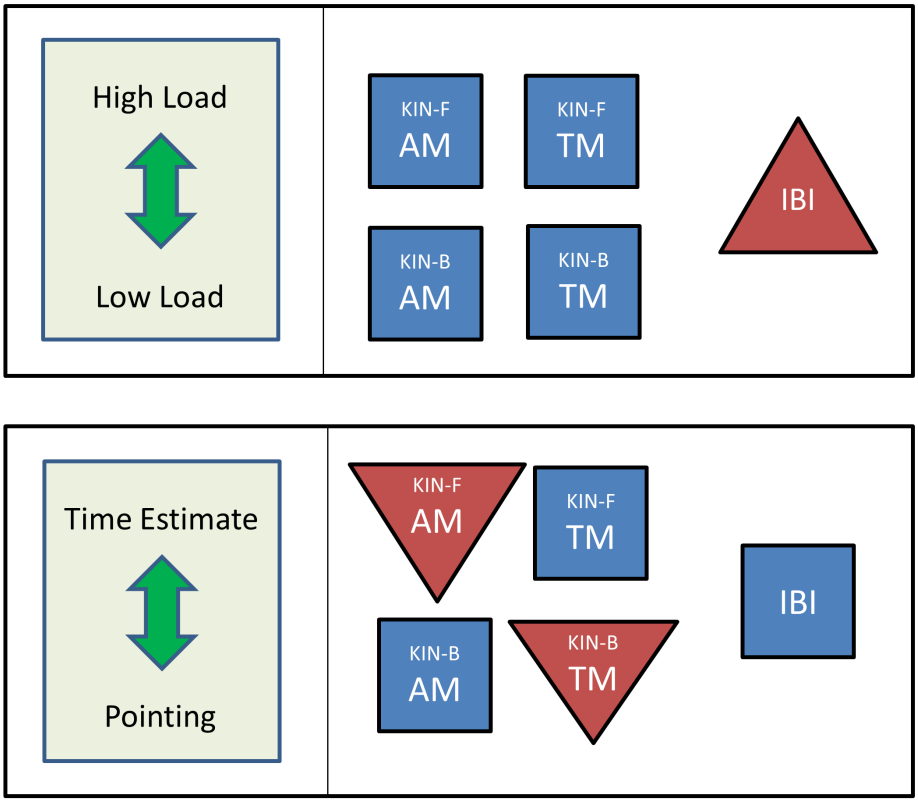

Figure 9. Summary of the statistical results (Top) Between the high and low-cognitive-load conditions, the statistics of the heart signal (IBI) significantly changed (signified in red upright triangle), such that signals were more predictive and less variable under the high-cognitive-load condition than under the low load condition. However, the statistics of motor signals (kinematics) for both forward and backward segments did not significantly change (signified in blue square). **(Bottom)** Between the pointing and time estimation task, the statistics of heart signals did not change significantly (signified in blue square). However, the statistics of the AM from the kinematics of forward segment ('KIN-F AM') and the TM from the kinematics of backward segment ('KIN-B TM') showed significant changes (signified in red inverted triangle), such that signals were more predictive and less variable during pointing tasks than during time estimation tasks.

Given that the CNS seems to steer goal-directed movements while the ANS drives the heart, it is possible that the changes in heart signals reflect the dynamics of a quantifiable relationship between these two systems. However, other hidden parameters may also play a role in the statistical shifts of the heart signal with varying levels of cognitive load. For example, arousal may have played a mediating role. In fact, all participants expressed challenges in

performing the task under the high-cognitive-load condition, where they were to count backwards. As such, the task may have induced stress and thus changed the level of arousal in their system. It is possible that arousal played a direct role on the heart signals while it played a minor role on the motor signals. One possible interpretation is that signals from the CNS (e.g., voluntary motor signals) may often be influenced by many factors, thus providing more flexibility and allowing for more variations before shifting its statistical signature. In contrast, it may be that signals from the ANS (e.g., heart signals) remain within a tighter range, and are more robust to change, responding mainly to primitive survival-related factors such as stress-induced shifts in arousal levels. Perhaps combining the heart signal with other physiological outputs (e.g., galvanic skin response) could clarify the effects of cognitive load on the motor system. Here, we learned that even a minor change in the cognitive task alters the variability of the heart's IBI in quantifiable ways. As such, we may be able to use this paradigm to study other aspects of performance, including a characterization of stress levels modulated by cognitive loads, and their influences on the motor signals. At the end, the susceptibility of the heart signal to stress may provide an outcome measure to assess the extent to which elevated levels of cognitive load may or may not disrupt behavioral performance.

As an alternative way of examining the effect of cognitive load, we gathered the statistics of the signals in response to two different tasks– the basic pointing task and the time estimation pointing task. Both tasks required the participant to make the same gesture of touching the display screen, but the time estimation task incurred higher cognitive load as the participant was simultaneously making a decision on the estimated time while touching the display screen.

During the time estimation task, the estimated Gamma PDF of the micro-movements harnessed from goal-directed forward segments, specifically the AM metric, showed to be less noisy (i.e., lower scale parameter) and more symmetric (i.e., higher shape parameter) than during the pointing task. The shift in the statistical signatures was consistent across all participants during the forward motions. For spontaneous backward segments, the same distributional shift of the fitted Gamma PDF was found in the signal's TM metric, such that there were less variability and more symmetry in the estimated PDFs during the time estimation task. Interestingly, participants did not explicitly express difficulty in performing the time estimation task relative to the pointing task. These tasks required the same biomechanical solution and were executed with the same arm-hand linkage. Pointing is a very automatic task, and yet several motor signals from the peripheral limbs were significantly affected. This implies involvement of the central controllers at the CNS level. Overall, these findings indicate that at the voluntary (forward) and automatic/spontaneous (backwards) levels of control, congruent changes in the statistics of spatio-temporal parameters of motor signals are found between the two tasks.

This finding has some parallel with previous findings on how the statistics of deliberate goal-directed motor signals (i.e., movement with a higher level of intent) are more predictive and less variable than spontaneous motor signals (i.e., movements with a lower level of intent) [4]. Since movements during the time estimation task required more cognitive focus than during the pointing task, and goal-directed movements required more focus than spontaneous movements, it may be that movements involving a high level of cognitive focus influence the statistics of motor signals to be less variable and more predictable. For future studies, it would

be helpful to examine the motor signals under differing levels of attentional focus with marked cognitive goals to verify whether this is indeed the case.

Overall, the results suggest that kinematic and autonomic parameters are sensitive to the level of cognitive loads. Indeed, these parameters may provide outcome measures of performance during tasks with varying degrees of cognitive loads.

4.2. Temporal and spatial metrics of micro-movement data

In analyzing the micro-movements of motor signals, their fluctuations were represented by two different metrics – AM and TM. AM represents the spatial aspect of movement, since speed profiles are a function of distance (i.e., space) over time, while the unit time remains constant in our case. Hence, the amplitude of speed profiles can simply be reduced to a function of distance. TM, on the other hand, represents the temporal aspect of movements. Overall, the spatial metric was informative in differentiating the levels of cognitive load between the pointing task and time estimation task for forward movements, while the temporal metric was more informative for backward movements. Given that the spontaneous/backward movement was not instructed to the participant, the forward movements may entail higher awareness about the ***external visual*** target than backward movements. In contrast, given that backward movements are automatically performed towards the body, they may entail a more ***internal proprioceptive*** awareness about the body position (so as to not hit the body on the way back from the target). As such, it is possible that the spatial statistics of forward reaches may be a better outcome measure of voluntary performance with higher awareness, whereas the temporal statistics of backward reaches may be more informative of spontaneous performance

under lower awareness. These hypotheses can be further tested in the future using the data from the postural domain, as another layer of internally generated variability.

Part of our interpretation of these results is that there may be a developmental explanation behind this finding. A newborn infant starts life with little *deliberate autonomy* and awareness of the body. At this nascent stage, the nervous system will react reflexively and will most likely rely on signals that are internally driven. This is because the infant has yet to develop vision and acquire the deliberate autonomy to maneuver the body at will within the external space. Consequently the nascent nervous system may primarily rely on internal signals. Because most movements at this stage are reflexive and spontaneous, thus involving a relatively low level of intent, the statistics of such micro-movements may be most informative from internally driven metrics, such as the TM. As an individual matures, the brain may rely more on external sources of sensory guidance in controlling one's movement. As such, movements directed at visual targets will become more deliberate and will necessarily involve a higher level of intent than spontaneous reflexes. Because goal-directed movements require the individual to understand one's body in relation to the external space, the statistics of such micro-movements may be most informative from externally driven sources, such as those based on spatial metrics (e.g., AM).

4.3. Embodied approach to studying cognition

To approach the study of cognitive performance, the current study employs a novel methodology. The new method extracts the signals obtained from the CNS and the ANS, and statistically characterizes those signals as a function of cognitive load to gain a glimpse into the

brain and body dynamics. In this sense, we characterized cognitive load with sensory and somatic-motor signals, alluding to processes that occur in a closed loop between the brain and the body. For instance, the input signals from the micro-movements of the motor and heart signals can be an important source of guidance to the brain, as they may be a form of feedback to help the brain compensate for synaptic transductions and transmission delays. By selectively shifting the signatures of statistical variability under different levels of cognitive load, different functional relations (maps) between bodily responses and environmental demands (including cognitive loads) may be built, to be able to predict ahead the consequences of bodily actions, even in the absence of or the intermittent availability of relevant sensory information.

This embodied approach to the study of cognitive processes has the potential to provide a more holistic perspective on our overall understanding of cognition and its development. Indeed, this simple paradigm was useful to examine the changes in bodily signals across multiple layers of the nervous systems, and characterize the sensory-motor behavior underlying cognitively driven performance. Furthermore, by adopting the kinesthetic reafferent framework in this study, we were able to capture the variations of motor and multifaceted sensory inputs that must be integrated to drive cognitive processes (e.g., selection, planning, decision making) under varying levels of control, ranging from voluntary to automatic to autonomic.

4.4. Individualized and empirical approach for biophysical data analyses

The methods presented in this study are aimed at transforming basic research in the cognitive and psychological science in three fundamental ways:

(1) By studying naturalistic behavior on a continuous timeframe, as opposed to constraining it to discrete events such as motion within epochs, mouse clicks, or hand coding of videos.

(2) By providing a more comprehensive, multilayered profiling of the nervous systems' activity underlying the execution of tasks with varying levels of cognitive load.

(3) By offering a new unifying statistical platform that enables a personalized assessment of behavior rather than adopting a "one-size-fits-all model" without empirical verification of assumed normality, linearity and stationarity in the biophysical data.

Here, the biorhythms of each individual are continuously profiled using the statistics of micro-movements with high-resolution instrumentation, and using an experimental paradigm that captures varying levels of control from different nervous systems. The work also offers an example of using a unifying statistical platform (SPIBA), which can be applicable across different tasks and instrumentations, and on different biophysical waveforms examined under a common standardized scale. We also show examples of an objective and personalized assessment of an individual, which can produce biometrics from naturalistic behaviors that can be easily translated from the lab to the home/clinical environment. As such, this approach invites further developments towards the new concept of precision medicine [33], and away from current behavioral assessments which tends to obstruct progress towards individualized targeted treatments. Precision medicine is a new approach in acquiring and integrating information from biomedical research and clinical practices, to develop therapies based on an individual's unique biological signatures. The present work is in line with the goals of precision medicine, as it moves beyond the "*one size fits all*" traditional model of behavior, and provides

new means to assess and dynamically track the single individual's performance across different naturalistic contexts.

Also, the methods used in this study adopt an empirical approach in analyzing data. Traditional researches have analyzed psycho-physiological data assuming that they were stationary and normally distributed, resulting in gross data loss. This is because the traditional approach tends to smooth out the variability that occurs from trial to trial and lump together individuals with different statistical signatures. However, the variability that is otherwise smoothed out as noise or treated as nuisance can be informative both at the individual and at the group level, as we have demonstrated here. Furthermore, the statistical shifts of metrics used in the current study can be examined on different time scales (e.g., minutes, days), making these a good candidate for outcome measures to dynamically track the evolution of the stochasticity of one's performance under different experimental conditions, behavioral treatments, or clinical interventions. As such, the methods can be used in longitudinal studies assessing a developmental progression or a pathological condition of certain nervous systems, and more generally in profiling neurotypical progression along an individual's lifespan.

Overall, the current study is a step forward from the traditional approach, as it analyzes physiological data on an individualized basis and empirically characterizes the variations in the nervous systems' performance in response to subtle manipulations.

4.5. Other clinical applications and limitations

The results showed that the micro-movement statistics of motor and heart signals are informative in characterizing cognitive load. The findings can be extended and applied to many

clinical situations. Since therapies involve cognitive load, it is possible that sometimes the treatments may be ineffective when the load is more than tolerable. In this case, the statistical metrics from the heart signals would be informative in keeping the treatments at its most effective level (e.g., lower stress level). Further, while some patients may benefit from external sources of sensory guidance, others may benefit instead from internal sources. As such, the methods provide the means to flexibly probe which parameters (externally driven *vs*. internally driven) may be most informative as outcome measures in maximally separating the effects of experimental manipulations within the lab or clinical interventions. In this sense, the metrics provided by the kinematics and heart signal outcomes can help in identifying the best treatments for the nervous systems to habilitate and rehabilitate motor control in tandem with cognitive performance.

The current study has several limitations:

(1) First, the results are based on merely nine healthy participants. To make a more robust conclusion about estimates of the population at large, more participants would need to be tested on, including individuals with pathological conditions affecting the heart and/or movements. This is because data obtained from healthy young individuals would be restricted to a particular range, while data from the patient population would provide us with value ranges closer to extreme cases. Indeed, combining various population groups would help in building a scale across the human continuum.

(2) As mentioned earlier, cognitive load is a multi-dimensional construct, so it needs to be probed using different means of sensory information beyond visual and auditory inputs. Moreover, increasing levels of cognitive load may not necessarily impact the statistics of

one's physiological signals in a linear fashion. For that reason, testing different types of cognitive load at varying degrees would be helpful to delineate important parameters of cognitive performance.

(3) We merely focused on the hand kinematics and the raw heart data but it is possible to study the internal representation of posture and muscle activity underlying the hand movements, as well as other signals from the ANS.

(4) The biophysical signals in the current results may have had a combined effect of arousal and cognitive load. Although these are different constructs, they may be confounded in various settings. It will be interesting to explore their relationship in future studies by measuring the arousal level and examining the kinematics and heart signals, because it is possible that the statistics of the heart signals are largely influenced by arousal that is induced by increased cognitive load. As such, it would be helpful to directly test the level of arousal to verify whether this is the case.

(5) Lastly, the proposed statistical platform makes a series of assumptions (e.g., independent and identically distributed events and focuses on the exponential family with additive statistics). While such assumptions enable a standardized metric to use across the population at large, including those with pathologies of the nervous systems, we may incur other forms of data loss. Future work will explore other statistical scenarios and further assess the variability of physiological and cognitive signals, using other types of processes to compare with the Gamma process.

4.6. Conclusions

The current study demonstrated interdependencies among signals from multiple layers of the nervous systems, through a proposed nervous systems architecture involving fundamentally different processes. The proposed processes are different in nature: deliberate, spontaneous and inevitable, thus encompassing very segregated types of activities with specific stochastic characteristics. Nonetheless, the interdependencies of signals during the experimental tasks designed for this thesis were clearly quantifiable and significant. These tasks, which required varying degrees of cognitive load, provide important evidence to justify the embodied approach to cognition. The thesis offers a new unifying statistical approach, data types and experimental paradigms to assess voluntary, automatic and autonomic signals through a common lens. As such this thesis provides tools to help advance the field of embodied cognition.

Appendices

A1. Four types of speed profile

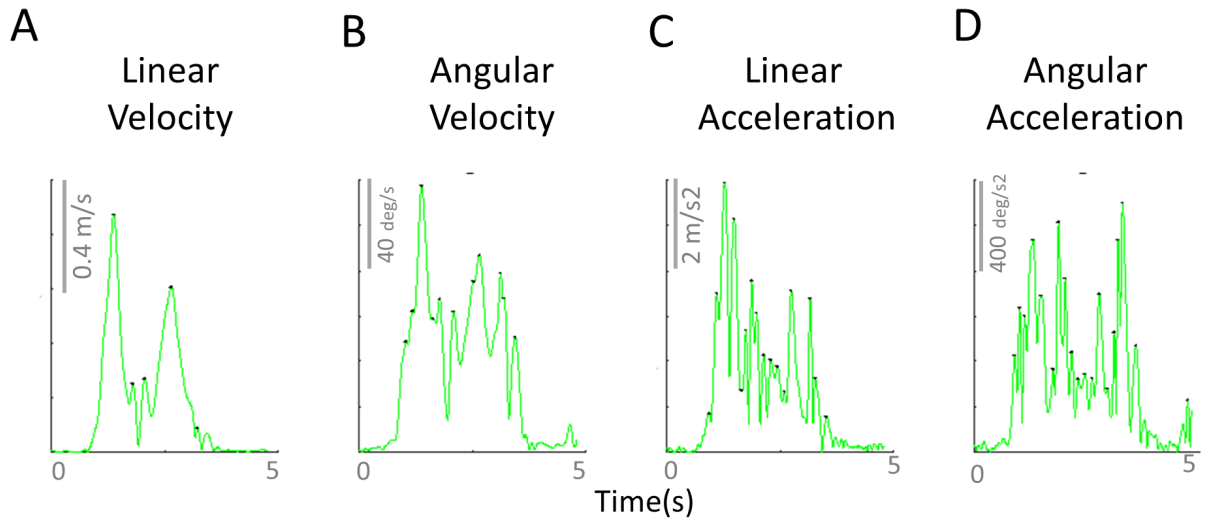

Figure A1. Four types of speed profile of a typical pointing movement. **(A)** Linear velocity **(B)** Angular velocity **(C)** Linear acceleration **(D)** Angular acceleration. Because angular acceleration showed to have the largest number of peaks during a single pointing movement, peak data obtained from the angular acceleration speed profile was analyzed, as this would provide the highest statistical power for the MLE process.

A2. MLE for kinematic parameters

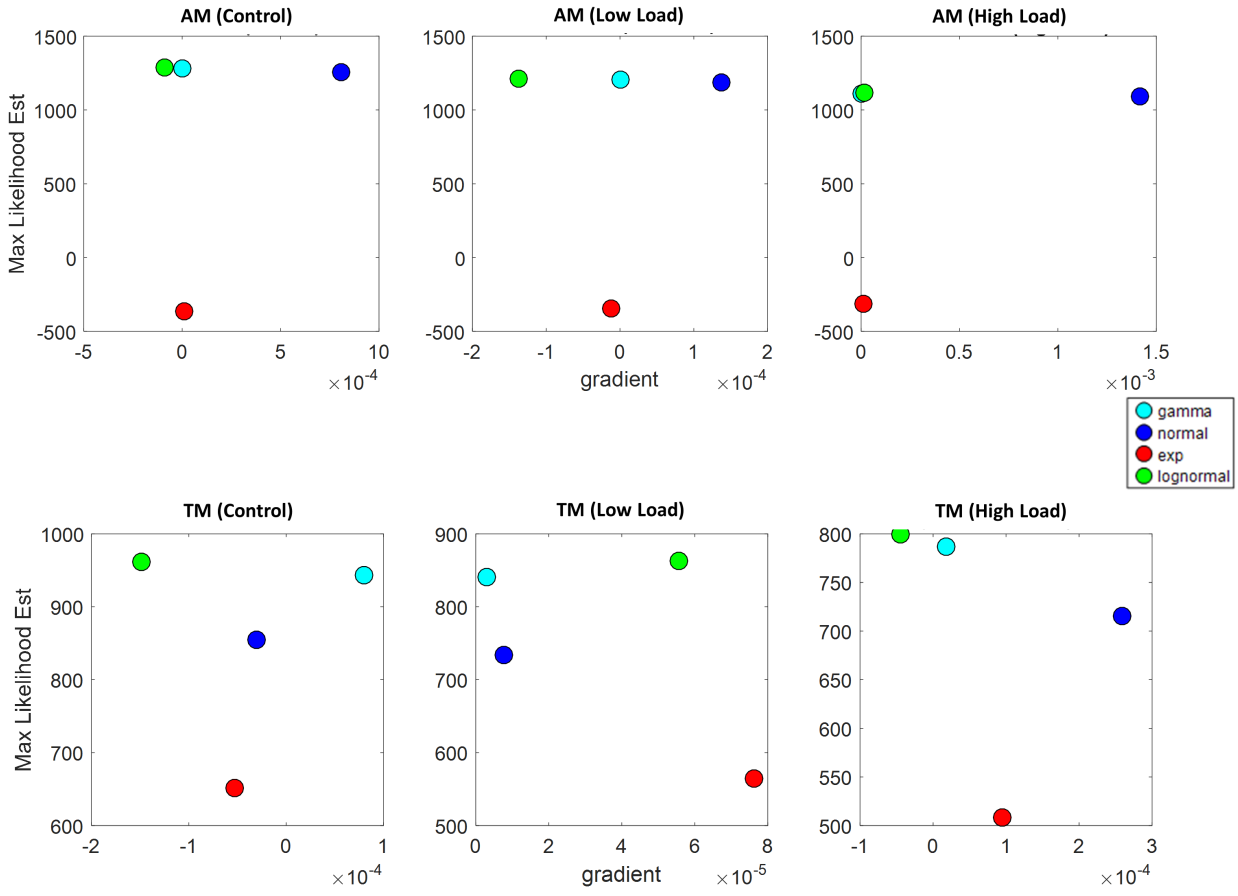

Figure A2. Maximum likelihood estimated values for AM index (top) and TM index (bottom) for 3 different conditions, for a typical participant. The horizontal axis contains the value of the gradient at the end of the optimization process ($-5x10^{-4}$ ~ $1.5x10^{-3}$ range according to the set tolerance value of 10^{-30} for the optimization process). The vertical axis contains the maximum likelihood estimation value for the Gamma, normal, exponential and lognormal distributions (see legend). The respective values are: AM for control condition [1279.0,1256.6,-366.9,1288.7], AM for low load condition [1203.9,1186.6,-345.2,1211.2], AM for high load condition [1111.0,1090.4,-314.2,1120.1], TM for control condition [943.4,854.7,651.7,961.3], TM for low load condition [841.1,733.5,564.9,863.4], TM for high load condition [787.1,715.0,508.7,799.7].

A3. MLE for inter-beat interval

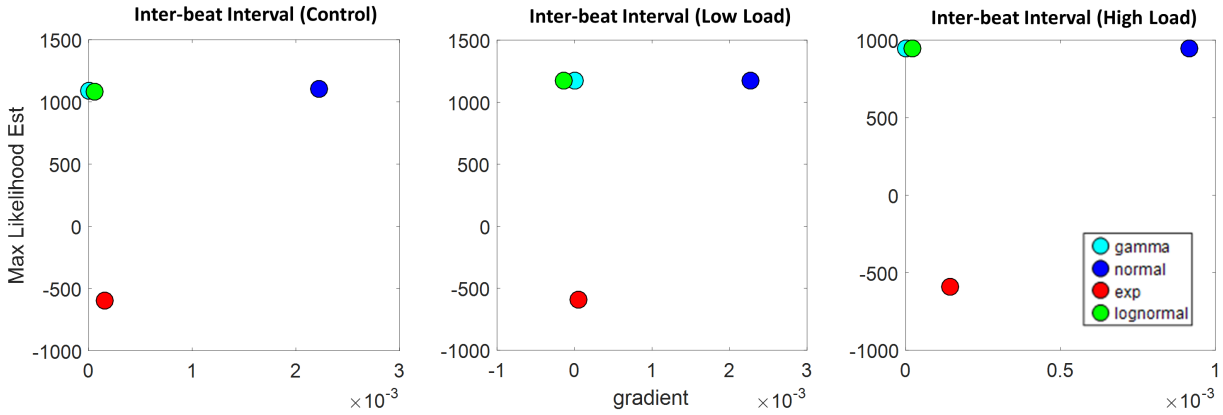

A3. Maximum likelihood estimated values for inter-beat interval for 3 different conditions, for a typical participant. The horizontal axis contains the value of the gradient at the end of the optimization process ($-1x10^{-3}$ ~ $3x10^{-3}$ range, according to the set tolerance value of 10^{-30} for the optimization process). The vertical axis contains the maximum likelihood estimation value for the Gamma, normal, exponential and lognormal distributions (see legend). The respective values are: control condition [1090.3,1100.8,-595.1,1083.9], low load condition [1175.9,1176.1,-590.1,1175.2], high load condition [946.75, 944.99, -589.92, 946.65].

A4. CNS voluntary control assessment under high- and low-cognitive-load conditions
FORWARD REACHES

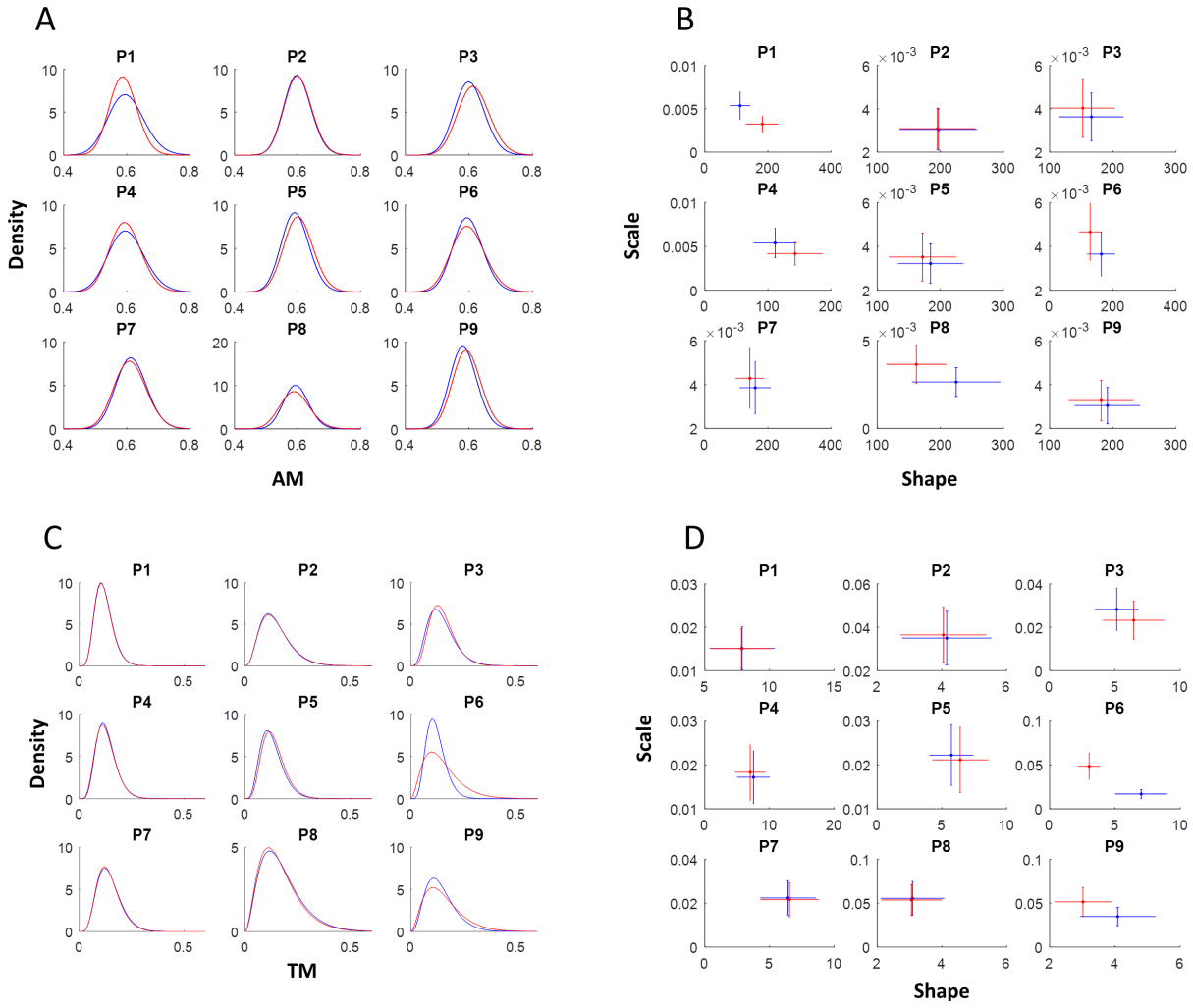

Figure A4. CNS voluntary control assessment under high- and low-cognitive-load conditions. Kinematics signals of the hand for goal-directed forward segments. **(A,B)** Estimated Gamma PDF and parameters of the AM and **(C,D)** TM for low-cognitive-load condition (blue) and high-cognitive-load condition (red) per participant (P1-P9). The estimated Gamma parameters for both metrics did not show a distinct trend in the separation between the two conditions.

A5. CNS automatic control assessment under high- and low-cognitive-load conditions

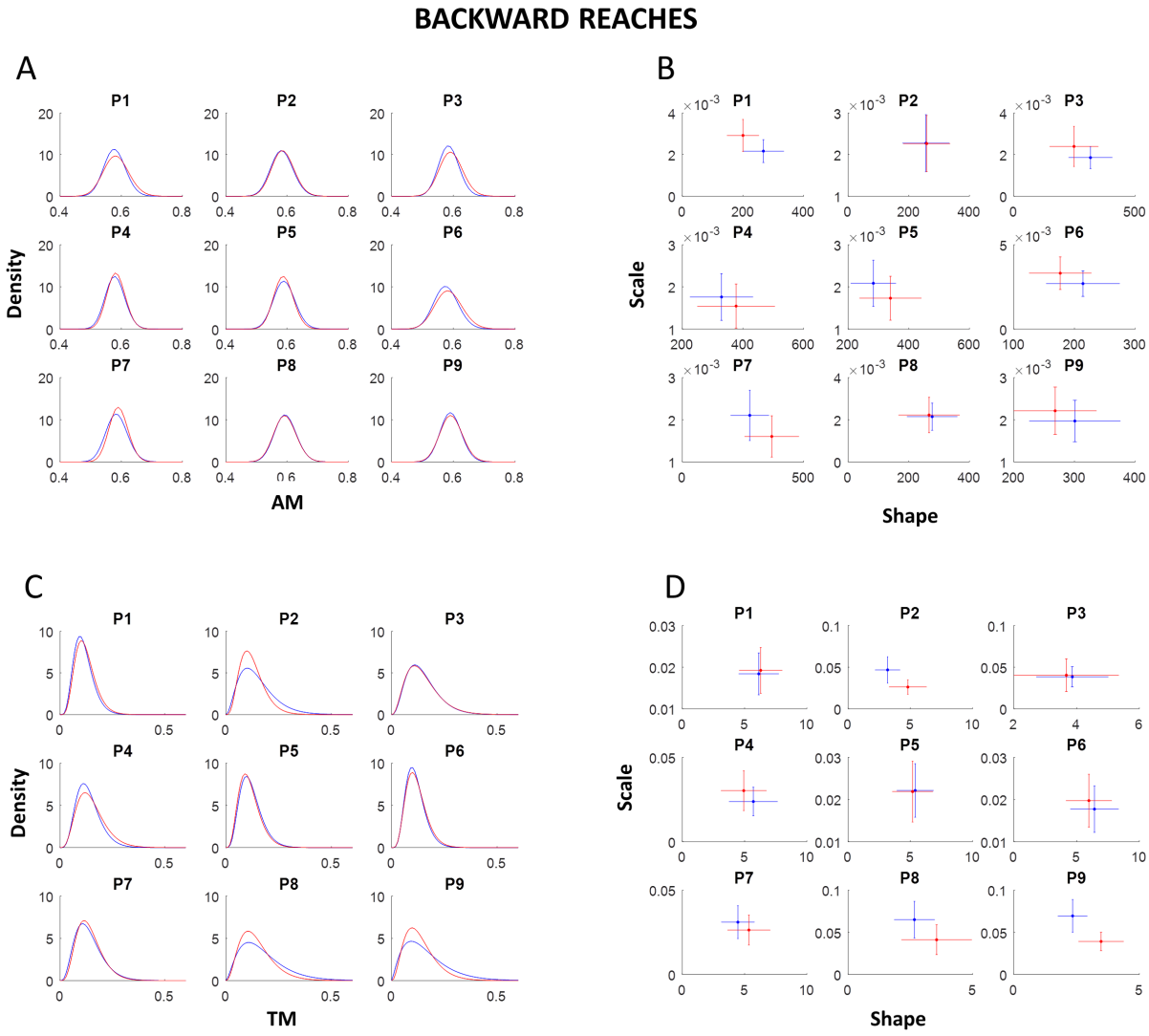

Figure A5. CNS automatic control assessment under high- and low-cognitive-load conditions. Kinematics signal of the hand for spontaneous backwards segments. **(A,B)** Estimated Gamma PDF and parameters of the AM and **(C,D)** TM for low-cognitive-load condition (blue) and high-cognitive-load condition (red) per participant (P1-P9). The estimated Gamma parameters for both metrics did not show a distinct trend in the separation between the two conditions.

A6. ANS autonomic control assessment during pointing and time estimation tasks

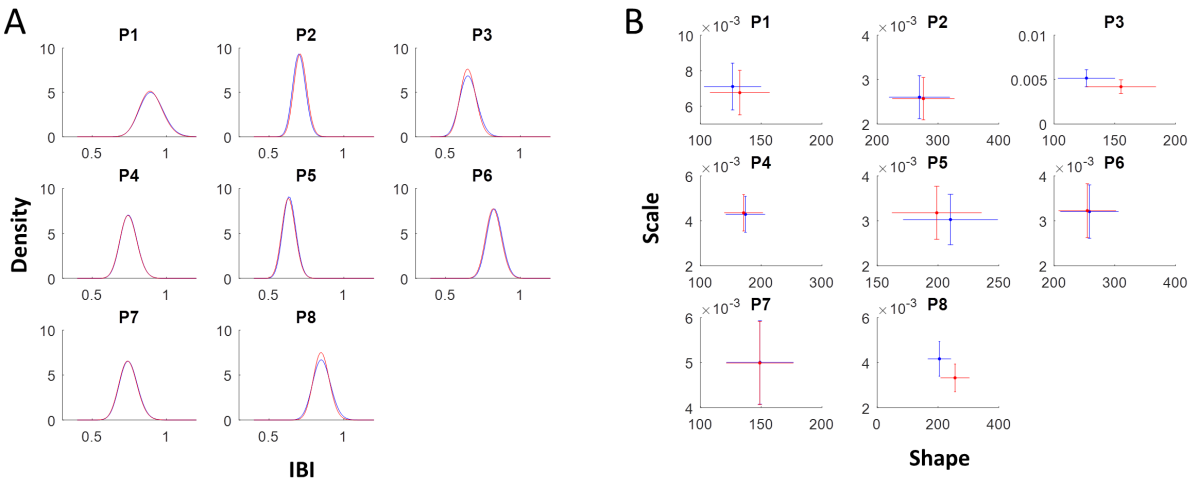

Figure A6. ANS autonomic control assessment under high- and low-cognitive-load conditions**. (A)** Estimated Gamma PDF and **(B)** parameters of IBI for the pointing task (blue) and time estimation task (red) per participant (P1-P8). The estimated Gamma parameters of the IBI probability distribution function did not show any separation between the pointing and time estimation task for all participants.

Table A1. Median time (ms) elapsed to complete a pointing gesture (composed of a forward and backward movement segment) for each condition

Participant	Low Load	High Load	Pointing	Time-Estimation
P1	1325	1535	1415	1405
P2	1570	1620	1675	1765
P3	1210	1740	1368	1340
P4	1475	1655	1483	1370
P5	1520	1535	1598	1510
P6	1190	1395	1445	1333
P7	1845	1943	1865	1985
P8	1405	1760	1750	1565
P9	1763	2145	1820	1770

Table A2. Comparison of micro-movement of motor signals between low vs. high cognitive load using Kruskal-Wallis non-parametric test

Participant	AM			TM		
	x^2	df	p-value	x^2	df	p-value
P1	1.91	(1,749)	0.17	0.02	(1,631)	0.88
P2	0.41	(1,643)	0.52	0.13	(1,524)	0.71
P3	17.89	(1,604)	<0.01**	3.95	(1,491)	0.05
P4	0.01	(1,648)	0.91	0.01	(1,529)	0.91
P5	10.32	(1,708)	<0.01**	4.77	(1,591)	0.03*
P6	0.34	(1,818)	0.56	4.73	(1,709)	0.03*
P7	2.86	(1,625)	0.09	0.17	(1,509)	0.68
P8	3.17	(1,676)	0.07	1.69	(1,579)	0.19
P9	11.52	(1,804)	<0.01**	1.63	(1,688)	0.20

References

1. Kawato, M. and D. Wolpert, *Internal models for motor control.* Novartis Found Symp, 1998. **218**: p. 291-304; discussion 304-7.
2. Wolpert, D.M. and M. Kawato, *Multiple paired forward and inverse models for motor control.* Neural Netw, 1998. **11**(7-8): p. 1317-29.
3. Wolpert, D.M., R.C. Miall, and M. Kawato, *Internal models in the cerebellum.* Trends Cogn Sci, 1998. **2**(9): p. 338-47.
4. Torres, E.B., *Two classes of movements in motor control.* Exp Brain Res, 2011. **215**(3-4): p. 269-83.
5. Torres, E.B., *Atypical signatures of motor variability found in an individual with ASD.* Neurocase: The neural basis of cognition, 2012. **1**: p. 1-16.
6. Torres, E.B., et al., *Autism: the micro-movement perspective.* Front Integr Neurosci, 2013. **7**: p. 32.
7. Von Holst, E. and H. Mittelstaedt, *The principle of reafference: Interactions between the central nervous system and the peripheral organs*, in *Perceptual Processing: Stimulus equivalence and pattern recognition*, P.C. Dodwell, Editor. 1950, Appleton-Century-Crofts: New York. p. 41-72.
8. Cole, J., *Pride and a daily marathon*. 1st MIT Press ed. 1995, Cambridge, Mass.: MIT Press. xx, 194 p.
9. Torres, E.B., J. Cole, and H. Poizner, *Motor output variability, deafferentation, and putative deficits in kinesthetic reafference in Parkinson's disease.* Front Hum Neurosci, 2014. **8**: p. 823.
10. Torres, E.B., *Signatures of movement variability anticipate hand speed according to levels of intent.* Behavioral and Brain Functions, 2013. **9**: p. 10.
11. Nguyen, J., et al., *Schizophrenia: The micro-movements perspective.* Neuropsychologia, 2016. **85**: p. 310-26.
12. Torres, E.B., *Signatures of movement variability anticipate hand speed according to levels of intent.* Behav Brain Funct, 2013. **9**: p. 10.
13. Torres, E.B., *New symmetry of intended curved reaches.* Behav Brain Funct, 2010. **6**: p. 21.
14. Torres, E.B., K.M. Heilman, and H. Poizner, *Impaired endogenously evoked automated reaching in Parkinson's disease.* J Neurosci, 2011. **31**(49): p. 17848-63.
15. Torres, E.B., *Atypical signatures of motor variability found in an individual with ASD.* Neurocase, 2013. **19**(2): p. 150-65.
16. Torres, E.B., et al., *Toward Precision Psychiatry: Statistical Platform for the Personalized Characterization of Natural Behaviors.* Front Neurol, 2016. **7**: p. 8.
17. Torres, E.B., P. Yanovich, and D.N. Metaxas, *Give spontaneity and self-discovery a chance in ASD: spontaneous peripheral limb variability as a proxy to evoke centrally driven intentional acts.* Front Integr Neurosci, 2013. **7**: p. 46.
18. Torres, E.B. and K. Denisova, *Motor noise is rich signal in autism research and pharmacological treatments.* Sci Rep, 2016. **6**: p. 37422.
19. Torres, E.B. and J.V. Jose, *Novel Diagnostic Tool to Quantify Signatures of Movement in Subjects with Neurological Disorders, Autism and Autism Spectrum Disorders*, R. University, Editor. 2012: US.
20. Paas, F.G., J.J. Van Merrienboer, and J.J. Adam, *Measurement of cognitive load in instructional research.* Percept Mot Skills, 1994. **79**(1 Pt 2): p. 419-30.
21. Tabbers, H.K., R.L. Martens, and J.J. van Merrienboer, *Multimedia instructions and cognitive load theory: effects of modality and cueing.* Br J Educ Psychol, 2004. **74**(Pt 1): p. 71-81.

22. Leppink, J., et al., *Development of an instrument for measuring different types of cognitive load.* Behav Res Methods, 2013. **45**(4): p. 1058-72.
23. Fredericks, T.K., et al., *An investigation of myocardial aerobic capacity as a measure of both physical and cognitive workloads.* International Journal of Industrial Ergonomics

2005. **35**(12): p. 1097-1107.
24. Ikehara, C.S. and M.E. Crosby. *Assessing cognitive load with physiological sensors*. in *Proceedings of the 38th annual Hawaii international conference on system sciences* 2005. IEEE.
25. Ryu, K. and R. Myung, *Evaluation of mental workload with a combined measure based on physiological indices during a dual task of tracking and mental arithmetic.* International Journal of Industrial Ergonomics, 2005. **35**(11): p. 991-1009.
26. Shi, Y., Ruiz,, et al., *Galvanic skin response (GSR) as an index of cognitive load*, in *CHI'07 extended abstracts on Human factors in computing systems* 2007, ACM. p. 2651-2656.
27. Haapalainen, E., et al. *Psycho-physiological measures for assessing cognitive load*. in *Proceedings of the 12th ACM international conference on Ubiquitous computing*. 2010. ACM.
28. Gallistel, C.R., *The importance of proving the null.* Psychol Rev, 2009. **116**(2): p. 439-53.
29. Raj, A.T., et al., *P-hacking.* J Contemp Dent Pract, 2017. **18**(8): p. 633-634.
30. Martin, G.N. and R.M. Clarke, *Are Psychology Journals Anti-replication? A Snapshot of Editorial Practices.* Front Psychol, 2017. **8**: p. 523.
31. Bruns, S.B. and J.P. Ioannidis, *p-Curve and p-Hacking in Observational Research.* PLoS One, 2016. **11**(2): p. e0149144.
32. Kathirvel, P., et al., *An efficient R-peak detection based on new nonlinear transformation and first-order Gaussian differentiator.* Cardiovascular Engineering and Technology, 2011. **2**(4): p. 408-425.
33. Hawgood, S., et al., *Precision medicine: Beyond the inflection point.* Sci Transl Med, 2015. **7**(300): p. 300ps17.
34. Gallistel, C.R. and A.P. King, *Memory and the computational brain : why cognitive science will transform neuroscience*. 2009, Chichester, West Sussex, UK ; Malden, MA: Wiley-Blackwell. xvi, 319 p.
35. Torres, E.B., et al., *Sensory-spatial transformations in the left posterior parietal cortex may contribute to reach timing.* J Neurophysiol, 2010. **104**(5): p. 2375-88.
36. Mosimann, J.E., *Size Allometry: Size and Shape Variables with Characterizations of the Lognormal and Generalized Gamma Distributions.* Journal of the American Statistical Association, 1970. **65**(330): p. 930-945.
37. Shimazaki, H. and S. Shinomoto, *A method for selecting the bin size of a time histogram.* Neural Comput, 2007. **19**(6): p. 1503-27.
38. Freedman, D. and P. Diaconis, *On the histogram as a density estimator: L theory.* Probability Theory, 1981. **57**(4): p. 453-476.
39. Torres, E.B., et al., *Characterization of the Statistical Signatures of Micro-Movements Underlying Natural Gait Patterns in Children with Phelan McDermid Syndrome: Towards Precision-Phenotyping of Behavior in ASD.* Front Integr Neurosci, 2016. **10**: p. 22.
40. Fano, U., *Ionization Yield of Radiations. II. The Fluctuations of the Number of Ions.* Physical Review, 1947. **72**(1): p. 26.
41. Kalampratsidou, V. and E.B. Torres. *Outcome Measures of Deliberate and Spontaneous Motions*. in *Third International Symposium on Movement and Computing, MOCO'16*. 2016. Thessaloniki, GA, Greece: ACM.

42. Kalmpratsidou, V. and E.B. Torres. *Invariant and variable relations emerge with degrees of difficulty within habitual and surprise touch-point motions*. in *Visual Science Society Annual Meeting*. 2014. Saint Pete's Beach, Tampa Bay, Fla.

Notes

https://www.google.com/patents/US20140336539